SES COLLEGE SREEKANDAPURAM

(Accredited by NAAC with 'B+' Grade) Affiliated to Kannur University

Criterion 3
Research,Innovation and Extension

3.3- Research Publication and Awards

3.3.2 Number of research papers per teachers in the Journals notified on UGC website

Polymer Bulletin
https://doi.org/10.1007/s00289-023-04945-9

ORIGINAL PAPER

Solid electrolyte membranes with Al_2O_3 nanofiller for fully solid-state Li-ion cells

Merin K. Wilson[1] · Cyril Augustin[1] · A. Abhilash[1] · B. Jinisha[1,4] · Aldrin Antony[1,2] · M. K. Jayaraj[3] · S. Jayalekshmi[1,2]

Received: 2 May 2023 / Revised: 20 July 2023 / Accepted: 6 August 2023

Abstract

Fully solid-state lithium-ion cells have the benefits of excellent safety, remarkable electrochemical stability, and extended cycle life. They are categorized as prospective candidates for new-generation energy storage devices capable of safe and stable operation for relatively long periods. In whole solid-state Li-ion cells, polymer-based solid electrolyte membranes (SEMs) are expected to serve as both the solid electrolyte and the partition material. Remarkably high ionic conductivity and efficient ion diffusion can be achieved in SEMs by incorporating inorganic filler materials. In the present work, solid electrolyte membranes are developed by a simple solution cast method. The addition of Al_2O_3 nanoparticles is found to enhance the ionic conductivity of SE membranes to 1.25×10^{-4} S cm^{-1} for optimum concentrations of lithium salt and filler material. These SE membranes show relatively high electrochemical stability window up to 4.75 V. Transparent and freestanding SE membranes developed using PEO-PVDF-$LiNO_3$-Al_2O_3 have excellent thermal stability, ideal ion transport number, and good electrochemical properties, suitable for applications in solid-state lithium-ion cells. Assembled $LiFePO_4$-MWCNT//SEM//Li metal half-cells are found to deliver an initial discharge capacity of 128 mAh g^{-1} at 0.1 C and an initial Coulombic efficiency of 98%.

Merin K. Wilson, Cyril Augustin have contributed equally to this work.

✉ S. Jayalekshmi
jayalekshmi@cusat.ac.in

[1] Division for Research in Advanced Materials (DREAM) Lab, Department of Physics, Cochin University of Science and Technology, Cochin, Kerala 682 022, India

[2] Centre of Excellence in Advanced Materials, Cochin University of Science and Technology, Cochin, Kerala 682022, India

[3] University of Calicut, Malappuram, Kerala 673 635, India

[4] Present Address: Department of Physics, SES College Sreekandapuram, Kannur 670 631, India

Published online: 08 September 2023

Graphical abstract

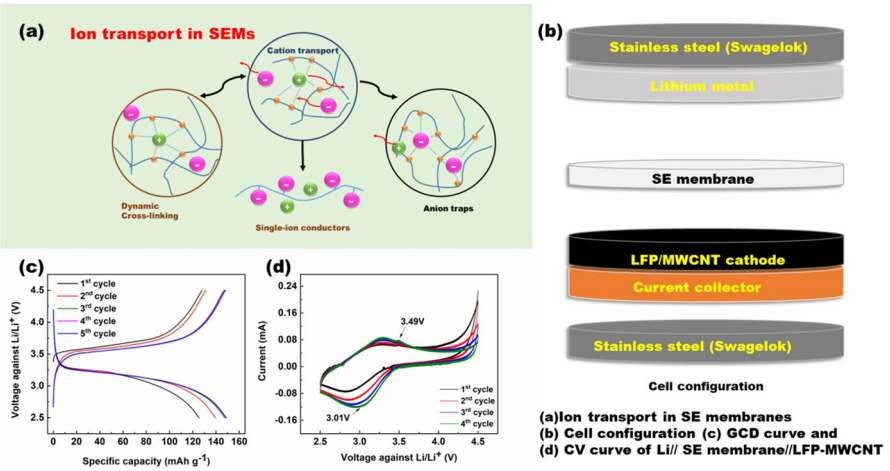

Keywords All-solid-state cells · Solid electrolyte membranes · Nanofiller · Transference number · Lithium-ion transport

Introduction

Lithium-ion cells are in solid demand in day-to-day life owing to their high value of energy density, output voltage, storage capacity, and long shelf life. They are extensively used for applications in portable electronic devices, power supplies, and hybrid electric vehicles [1]. Research on Li-ion cells has recently been intensified in identifying novel materials to serve as solid electrolytes. The use of liquid electrolytes in conventional Li-ion cells has many inherent disadvantages. The possibility of electrolyte leakage, and the associated short-circuiting, and fire hazards make it mandatory to have robust sealing for the cells, which complicates cell design, especially for bigger ones [2]. Another prime disadvantage of the commonly used liquid electrolyte, $LiPF_6$, in Li-ion cells is its sensitivity to impurities [3]. $LiPF_6$ decomposes to LiF and PF_5 at high temperatures, and decomposition to HF and PF_3O occurs in moist atmosphere at lower temperatures. The high reactivity of HF and PF_3O toward electrode materials is one of the major concerns. A solid LiF layer formed on the electrode surface, termed as solid electrolyte interface (SEI), functions as a shielding insulating layer [4]. These limitations can be avoided if suitable solid electrolytes can replace liquid ones. Among solid electrolytes, polymer-based solid electrolyte membranes (SEMs) have drawn intense research interest for energy storage device applications, mainly due to their flexibility, porosity, and the possibility of growing them as freestanding films and membranes [5–7]. For synthesizing polymer-based SEMs with anticipated lithium-ion conductivity, excellent compatibility between chosen polymers and inorganic salts and their dissociated

ions is mandatory, and these polymers are expected to afford a linked polar domain to facilitate free conduction pathways. There should not be any strong interaction between polymers and carrier ions to inhibit complete trapping of carrier ions [8]. Developing nanoparticles incorporated, polymer-based, composite SEMs offers one of the most viable approaches [9]. Polymer matrix, inorganic salt, and nano-sized filler material constitute the prime components of SEMs [10].

Various types of polymers, including polyethylene oxide (PEO), poly methyl methacrylate (PMMA), polyvinyl pyrrolidone (PVP), and polystyrene maleic anhydride (SMA), have been subjected to extensive investigations to assess their electrochemical performance [11]. High molecular weight, dielectric polymer, and polyethylene oxide (PEO) can be identified as one of the most promising polymers due to its high mechanical, chemical, and interfacial stability against lithium metal [12]. The presence of ether linkages with oxygen atoms placed at suitable inter-atomic separation, facilitating the segmental motion of the polymeric chain and consequently improving ionic conduction [13], helps to solvate different varieties of lithium salts. It has a partially crystalline structure, which is considered a barrier for high ionic conductivity. Polymer chain mobility can be improved by suppressing the crystalline nature of the polymer chain. The most viable approach to enhance the amorphous phase of PEO is to blend it with other suitable polymers [14–16]. The strong electron withdrawing group ($-CF_2-$) in the backbone of the polymer chain of PVDF can facilitate better intermolecular interactions [17]. Sites of C − F groups of PVDF-based electrolytes serve as binding locations for ions during ion transfer. In an electric field, these ions travel from one place to another or jump from one chain to another [18]. Lithium nitrate ($LiNO_3$) is endowed with low lattice energy of 808 kJ mol^{-1}, excellent thermal stability, and low hygroscopicity, which are advantageous for enhancing charge carrier density and handling the salt under ambient conditions [19]. Processes of breaking/forming ion-dipolar bonds between Li^+ ions and the functional groups of the host polymer and the associated intra- and inter-chain hopping constitute ion transport mechanisms in polymer blend-based electrolytes. Reasonable extent of the amorphous phase of SEMs is crucial to facilitate high polymer chain flexibility and faster segmental dynamics, which serve as the prime factors to trigger faster ion transport processes and enhance the ionic conductivity of the SEMs [20]. The different types of ionic conduction mechanisms in SEMs are schematically shown in Fig. 1.

Usually, solid electrolytes exhibit poor ionic conductivity at room temperature in the order of 10^{-5} Scm^{-1}. Hou and co-workers have developed a $LiPF_6$-containing polymeric, concentrated quasi-solid electrolyte having a remarkable electrochemical stability window of 5.5 V vs. Li/Li^+ and an ionic conductivity of 3.1×10^{-4} S cm^{-1} at 25 ℃ for lithium metal batteries [21–23]. By incorporating inert, ceramic oxide nanofillers like titanium dioxide (TiO_2), aluminum oxide (Al_2O_3), silicon dioxide (SiO_2), zirconium dioxide(ZrO_2), barium titanate ($BaTiO_3$), antimony trioxide (Sb_2O_3) and tin oxide (SnO_2), ionic conductivity and electrochemical properties of the SE membranes can be significantly improved [24]. By hindering the recrystallization affinity, nanofiller material destroys the crosslinking and dense packing of the polymer, which provides a favorable conduction path for ion migration. Surface charges on the nanofiller material bring about the dissociation of ion pairs which,

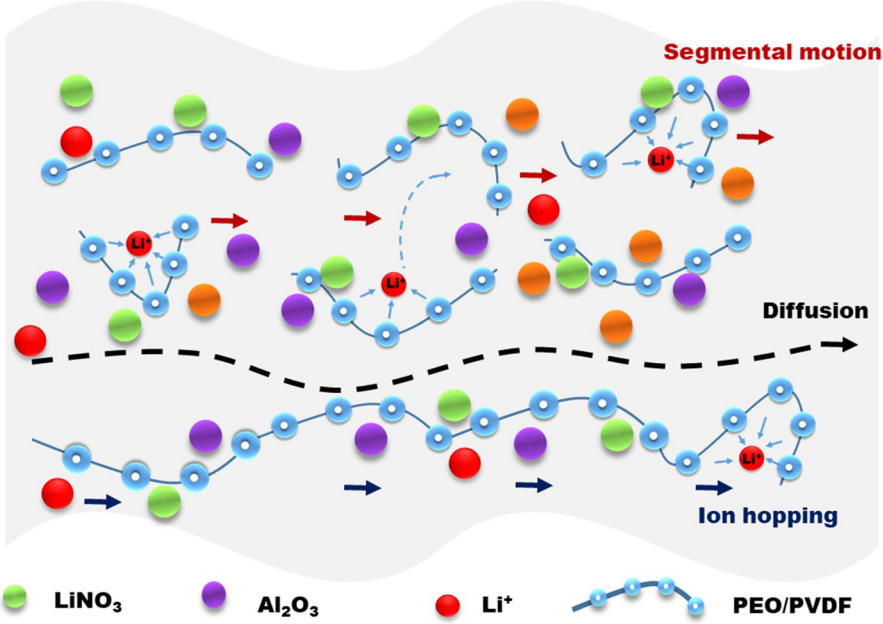

Fig. 1 Schematic illustration of different type mechanisms of ion transport in polymer-based nanocomposite solid electrolytes

along with flexible polymer segmental motion, are promoted by polymer dipole orientation which is significantly influenced by the presence of fillers in the host polymer matrix [25]. The amorphous nature of the host polymer is consequently enhanced by effectively reducing the recrystallization rate and lowering the glass transition temperature (T_g), which improves interfacial stability, ionic conductivity, and cation transport number [26].

Surface functionalization of the polymer blend occurring in the presence of filler Al_2O_3, with the formation of O/OH groups at the grain boundaries, facilitates hydrogen bonding with the moving ionic species, which results in enhancement of ionic conductivity of the SE membranes [27]. The increase in ionic conductivity can be related to Lewis acid–base type interactions of conducting species with the surface groups of the nanofiller, which decrease the polymer reorganization tendency and modify the polymer chain arrangement [28]. After incorporating Al_2O_3 nanofiller into the polymer matrix at low nanofiller concentrations (1 wt.%—10 wt.%), the system's physical, thermal, mechanical, and dielectric properties have been found to improve [29]. High filler loading affects the processability, mechanical strength, and flexibility of polymer composites. Moreover, the inorganic filler's poor compatibility with the polymer matrix causes weak interfacial adhesion and filler aggregation, resulting in high dielectric loss and low breakdown strength [30]. In the present work, good-quality SE membranes are grown by optimizing lithium salt, $LiNO_3$ concentrations in the polymer blend of PEO with PVDF. γ-Al_2O_3 is added as the filler material to the PEO-PVDF hybrid polymer blend, treated with $LiNO_3$ as lithium salt, to attain enhanced ionic conductivity

with better mechanical strength. Prototype fully solid-state cells are assembled in half-cell configuration using these SEMs against $LiFePO_4$-MWCNT as cathode. After 100 cycles, the cells are found to deliver a discharge capacity of 108 mA h g^{-1} and a charge capacity of 100 mA h g^{-1} with a capacity retention of 84% at 70 ℃ at a current rate of 0.1 C.

Experimental

Materials

The materials, polyethylene oxide (PEO; 200,000 g mol^{-1}), polyvinylidene fluoride (PVDF; 40,000 g mol^{-1}), lithium nitrate ($LiNO_3$; 68.95 g mol^{-1}), and aluminum oxide (Al_2O_3; 101.96 g mol^{-1}), obtained from Sigma – Aldrich were used for the synthesis of SE membranes. Using the solution casting method, flexible, transparent, and free-standing SE membranes were obtained. Iron oxalate dihydrate ($FeC_2O_4.2H_2O$; 143.91 g mol^{-1}), ammonium dihydrogen phosphate ($NH_4H_2PO_4$; 115.03 g mol^{-1}), and citric acid (HOC $(CH_2CO_2H)_2$; 192.124 g mol^{-1}) obtained from Sigma-Aldrich were used as received. Solvent dimethyl formamide (DMF) and HNO_3 (nitric acid) purchased from Merck Life Science private limited and multiwalled carbon nanotubes (MWCNT) purchased from Graphene supermarket were used for the synthesis of $LiFePO_4$/multiwalled carbon nanotubes composite cathode material. $LiFePO_4$/MWCNT composite cathode was synthesized by sol–gel method, and active material was obtained in powder form. DMC(dimethyl carbonate) obtained from Sigma-Aldrich was used as received for electrode cleaning in post-mortem analysis.

Synthesis of polymer-based, solid electrolyte membranes (SEMs)

Fixed concentrations of PEO (70%) and PVDF (30%) were dissolved in dimethyl formamide (DMF) with continuous stirring to get the PEO-PVDF polymer blend solution (15 mL). The ratio of PEO and PVDF was kept constant throughout the experiment. It is essential to observe that PVDF takes the role of a binder to assist in incorporating the lithium salt into the polymer blend matrix. Different weight percentages of the lithium salt, $LiNO_3$ (4, 8, 12, 15, and 20), were added to the polymer blend solution and stirred vigorously at 800 rpm for 12 h at room temperature under ambient air. Then solid electrolyte membranes were synthesized by adding 0.5, 1, 2, 3, and 4 weight% of Al_2O_3 nanofiller with fixed lithium salt (12 weight% of $LiNO_3$) concentration. The subsequent solutions were poured onto a Teflon petri-dish for drying under vacuum for 24 h at 50 ℃. Flexible, freestanding, and transparent SE membranes were peeled out from the petri-dish after evaporating the solvent [31].

Electrode preparation and cell assembly

$LiFePO_4$ was synthesized by sol–gel process, using precursors $LiNO_3$, iron oxalate dehydrate, and ammonium dihydrogen phosphate, which were dissolved in 1 M

HNO_3 solution. Citric acid was used as a chelating agent. The resulting gel was dried at 80 ℃ in a vacuum oven and then annealed at 700 ℃ in argon atmosphere. $LiFePO_4$/MWCNT nanocomposite cathode was obtained by physically mixing (by hand) $LiFePO_4$ and MWCNT using mortar and pestle and then sintering at 300 ℃ under argon. A slurry was prepared using active material $LiFePO_4$/MWCNT nanocomposite (0.16 g), polyvinylidene fluoride (0.02 g) (PVDF) as a binder, and carbon black (0.02 g) as a conductive additive in 80:10:10 ratio using N-methyl pyrrolidone (NMP) as solvent and was coated on aluminum foil by spray coating. These coated electrodes were dried in a vacuum oven at 60 ℃ overnight. Small circular disk-like electrodes of diameter 10–12 mm with mass loading of 2–3 mg cm^{-2} and 12–14 mm size SE membranes were used for the cell assembly. Fully solid-state test cells were assembled in half-cell configuration against lithium metal using Swagelok-type cells in an argon-filled glove box with a moisture level of less than 5 ppm, using SE, serving both as solid electrolyte and separator.

Characterization techniques

Structural, morphological, and thermal studies

Structural details of the SE membranes were explored by XRD analysis using Rigaku Max C diffractometer with Ni-filtered Cu Kα radiation of 1.54 Å. FTIR spectroscopic studies conducted using IR AFFINITY-1 CE, SHIMADZU spectrophotometer in the 400–4000 cm^{-1} range establish the complex formation between the polymer blend and the lithium salt. Raman spectral data was collected using Horiba LabRam HR spectrometer having 514 nm argon ion laser of 15 mW power as the radiation source. Morphological details of the SE membranes were assessed by electron microscopy using Jeol/ JEM 2100 microscope and Carl Zeiss Sigma FESEM instrument. Mechanical properties of the SE membranes were investigated using the machine UTM SHIMADZU 5kn, Japan. The thermal stability of the membranes was studied by Thermo-gravimetric analysis using Perkin Elmer STA 6000 instrument from room temperature to 700 ℃ under a controlled nitrogen atmosphere. For all the membrane samples, differential scanning calorimetry (DSC) measurements were conducted to determine the glass transition temperature and assess the flexibility of polymer chains, at a heating rate of 10 °C per minute from − 90 °C to 100 °C under nitrogen using Mettler Toledo DSC 822E.

Electrochemical studies

Ionic transport properties of the SE membranes were studied, employing an HP4192A impedance analyzer in the frequency range from 5 Hz to 13 MHz by sandwiching the SE membrane across stainless steel (SS) blocking electrodes using Swagelok-type cells [20]. Temperature dependence of ionic conductivity of SE membranes was studied in the temperature range from 303 to 343 K [27]. The total ionic transport number of the SE membranes was measured using Wagner's DC polarization method, by applying a fixed DC voltage (0.5 V) across the SS//SEM//

SS structure, where SS is stainless steel, acting as blocking electrodes [8]. Evans and Vincent's method [30] was used to determine the lithium-ion transference number. Symmetrical designs having Li//SE membrane//Li configuration were assembled in an argon-filled glove box. Using Biologic SP 300 potentiostat, cyclic voltammetry (CV) and linear sweep voltammetry (LSV) studies were carried out to investigate the electrochemical properties and fix the stability window of the SE membranes. Fully solid-state prototype cells were assembled in an argon-filled glove box using synthesized $LiFePO_4$ (LFP)-multiwalled carbon nanotubes (MWCNT) nanocomposite as cathode material, SE membrane as solid electrolyte (without separator) and Li metal as anode in half-cell configuration and galvanostatic charge–discharge (GCD) studies were carried out using eight-channel Battery Analyzer (0.002–1 mA, 5 V), provided by MTI corporation.

Results and discussions

XRD plot (Fig. 2) of PEO shows sharp peaks at about 19.2° and 23.2° in line with the crystalline property of PEO, related to (120) and (010) reflections of the monoclinic crystal system [32]. Broad peaks are also observed in the range of 25°–80°, representing the amorphous nature of PEO [33]. High amorphous content in PVDF is evident from its XRD plot. The strong peak at 20.3°, in the plot, can be related to (200) and the one at 18.1° to (110) planes, which can be attributed to reflections in β and α phases, respectively. More polar property is observed in the β phase than α phase [34]. Variation of the percentage of crystallinity of SE membranes on adding Al_2O_3 is shown in Fig. 2c. From the XRD pattern of the as-prepared $LiFePO_4$, demonstrated in Fig. 2d, the triphylite $LiFePO_4$ has an orthorhombic lattice structure and is a member of olivine family of lithium ortho-phosphates (JCPDS card No: 40–1499).

Characteristic Raman peaks (Fig. 3a) of PEO are observed at 1485 cm^{-1} (bending mode of CH_2), 1280 cm^{-1} (CH_2 symmetric stretching mode), 1232 cm^{-1} (CH_2 asymmetric stretching mode), and 1066 cm^{-1} (C–O–C stretching). The band at 844 cm^{-1} is assigned to CH_2 rocking mode, and the intensity of this band is related to the degree of crystallinity [35]. The highly intense SE mode at 845 cm^{-1} of PVDF is due to out-of-phase CF_2 stretching mode, and PVDF consists mainly of an amorphous β phase [36]. In the Raman spectrum of $LiNO_3$, a strong peak is observed at 1071 cm^{-1} due to the presence of anion $(NO_3)^-$. Presence of such $(NO_3)^-$ anions in the polymer matrix is reported to improve the amorphous nature of the host polymer [37].

In the PEO FTIR spectrum (Fig. 3b), the peak at 841 cm^{-1} represents the antisymmetric stretching mode of the CH_2 group, and the one at 955 cm^{-1} is attributed to C–O stretching vibration [38]. The broad peak at 1100 cm^{-1} is assigned to the C–O–C stretching mode of pure PEO. Vibrational bands of PEO at 1237 cm^{-1},1282 cm^{-1},1342 cm^{-1}, and 1466 cm^{-1} correspond to CH_2 symmetric twisting, CH_2 asymmetric twisting, CH_2 bending, and C–H bending of CH_2, respectively [39]. 1799 cm^{-1}, a small peak is observed, corresponding to an ether oxygen group of PEO [40]. The peak at 1402 cm^{-1} in the spectrum of PVDF is assigned to

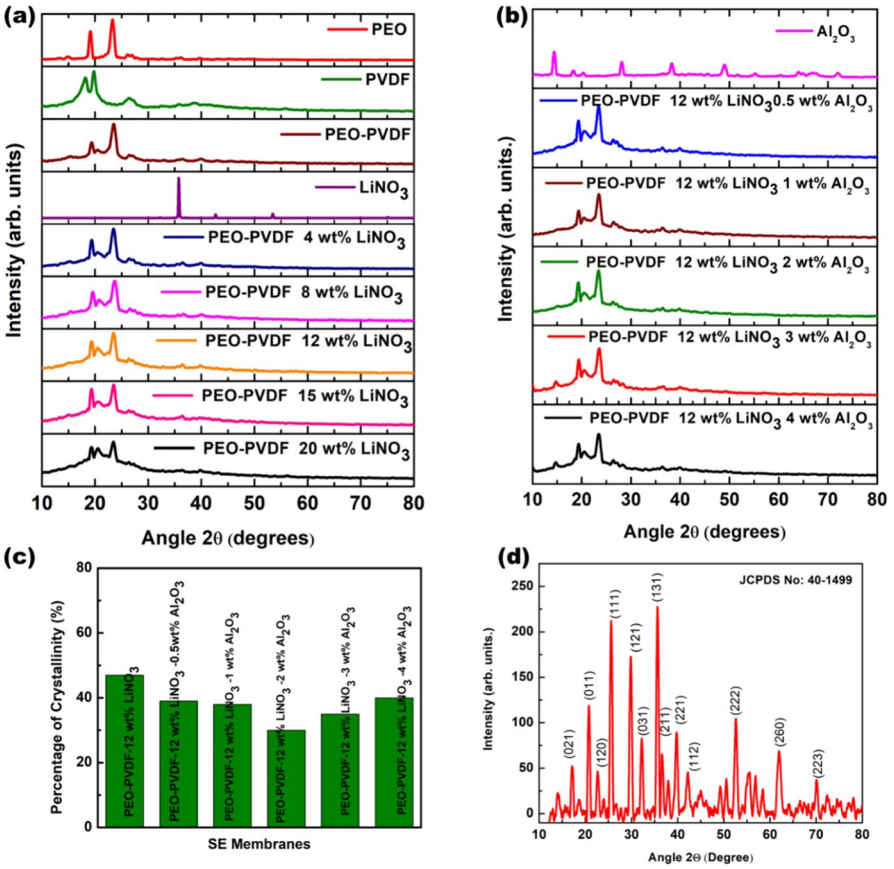

Fig. 2 XRD patterns of **a**, **b** PEO, PEO-PVDF polymer blend, $LiNO_3$salt, Al_2O_3, and solid electrolyte membranes **c** Histogram showing the variation of percentage of crystallinity of SE membranes **d** XRD pattern of LFP in accordance with JCPDS card No: 40–1499

C–F stretching vibration. Vibrational bands at 1175 cm^{-1} and 1216 cm^{-1} correspond to stretching frequencies of CF_2 and C–F, respectively, and the mode at 874 cm^{-1} is ascribed to vinylidene ($-C=CH_2$) group vibration [41]. Crystalline and amorphous peaks in PVDF are represented as peaks at 1069 cm^{-1} (α phase) and 828 cm^{-1} (β phase), respectively. Absorption bands of $LiNO_3$ at 1052 cm^{-1}, 1384 cm^{-1}, and 827 cm^{-1} are attributed to the symmetric stretching mode, asymmetric stretching mode, and out-of-plane deformation mode of NO_3^- ions [15]. On the addition of 12 weight% of $LiNO_3$ to the PEO-PVDF polymer blend, the intensity of the peaks at 1100 cm^{-1}, 955 cm^{-1}, and 841 cm^{-1} of PEO gets enhanced due to stretching of helical confirmation of PEO. The amorphous peak of PEO at 1100 cm^{-1} corresponding to C–O–C vibrational mode becomes significantly broader. It gets downshifted to 1087 cm^{-1}, and its crystalline phase shoulder peaks at 1056 cm^{-1} and 1144 cm^{-1} have almost disappeared, confirming the existence of solid ion–dipole coordination

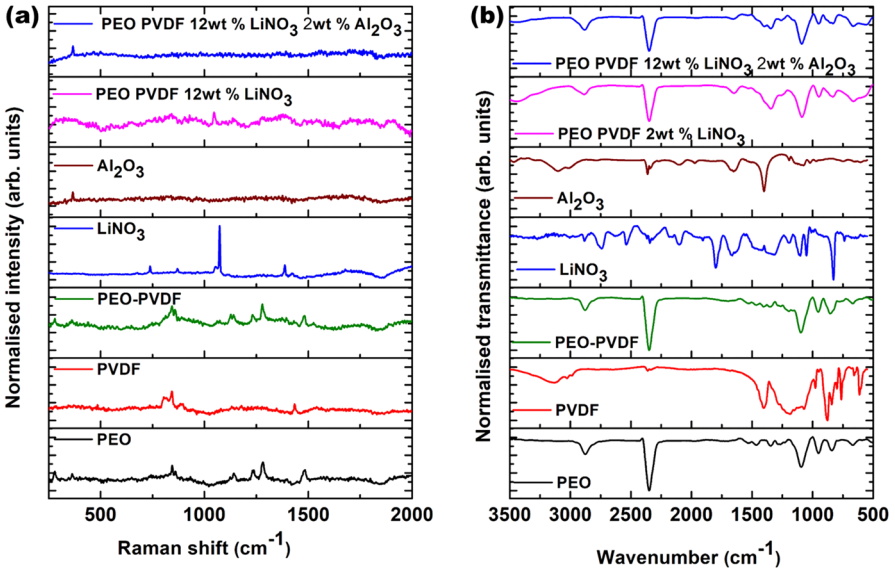

Fig. 3 **a** Raman spectra and **b** FTIR spectra of PEO, PVDF, PEO-PVDF polymer blend, $LiNO_3$ salt, Al_2O_3, SE membranes with 12 weight% of $LiNO_3$, and SE membrane with 12 weight% of $LiNO_3$ and 2 weight% of Al_2O_3

(O^-–Li^+) [42]. Due to ion–dipolar interactions, the C–O–C group's crystalline phase is significantly disrupted in the SE membranes. Doublet characteristic peaks at 1361 and 1339 cm^{-1} of CH_2 wagging mode merge into a single peak at 1360 cm^{-1} with a significantly reduced intensity, confirming the suppression of the PEO crystalline phase in SE membranes.

Stress–strain curves and variation of Young's modulus of different membranes are shown in Fig. 4a, b. On the addition of PVDF, the PEO membrane's tensile strength (3.5 MPa) is increased to 7.5 MPa. Here PVDF acts as a binder and strengthens the PEO membrane by forming the polymer blend. Mechanical strength gets significantly improved by the addition of the filler to the polymer electrolyte, and there is an increase in Young's modulus from 0.015 MPa for the PEO-PVDF-12 wt% of $LiNO_3$ -based SE membrane to 0.18 MPa for the PEO-PVDF-12 weight% of $LiNO_3$- 2 weight% of Al_2O_3 -based SE membrane. All the membranes show elastic behavior without obvious yield points before the breaks. Also, the values of stress and strain at break slightly get increased.

From TGA curves (Fig. 5a) for pure PEO, there is a plateau indicating minimal weight loss and good thermal stability up to 380 ℃, and the sample gets completely dissociated at 430 ℃. The small loss observed during the initial stages is due to moisture absorbed on the surface and residual solvent trapped in the micro-pores of the SE membranes. Compared with PEO-based polymer systems, thermal stability is enhanced significantly for the SE membranes by adding Li salt and ceramic fillers. The decomposition temperature observed for the SE membrane in the present work is considerably higher than that of liquid

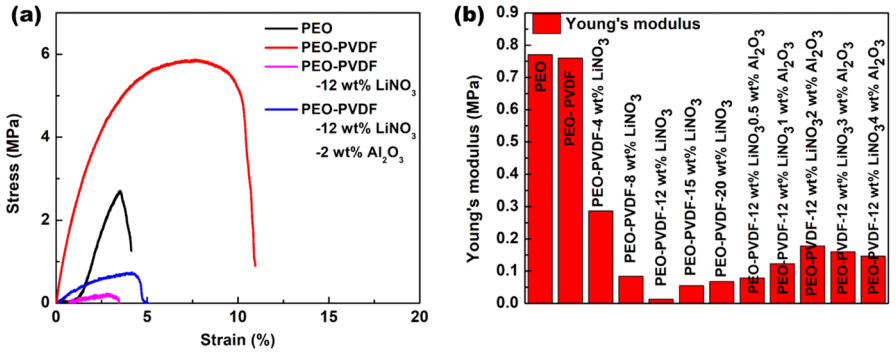

Fig. 4 **a** Stress–strain curves of PEO, PEO-PVDF polymer blend, PEO-PVDF polymer blend with 12 weight% $LiNO_3$, PEO-PVDF polymer blend with 12 weight% $LiNO_3$ and 2 weight% Al_2O_3 and **b** Variation of Young's modulus of different membranes

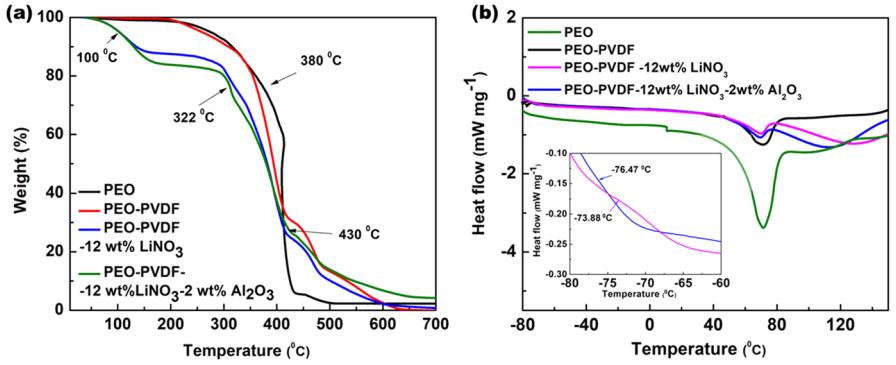

Fig. 5 **a** TGA curves and **b** DSC curves (inset; glass transition temperature)

electrolytes currently employed in Li-ion secondary cells. Homogeneous dispersion of Li salt and ceramic or filler in the polymer blend matrix can prevent the quick expansion of heat into the polymer blend system by slowing down the thermal degradation of SE membranes [43].

Glass transition temperature T_g of a polymer is concerned with the mobility of polymer chains, and lowering T_g indicates chain relaxation in the polymer system leading to increasing the amorphous nature, which promotes the enhancement of ion conduction [44]. For pure PEO, the T_g value is − 65.12 ℃, as per previous reports [45]. In the PEO-PVDF blend, the Tg value is shifted to − 67.55 ℃, and it again gets shifted to −73.88 ℃ with the addition of lithium salt. After adding inert filler Al_2O_3, T_g shows the lowest value of −76.47 ℃. The lowering of T_g values is attributed to the lowering of crystallinity, and % crystallinity is determined using the values of melting enthalpy of the samples [46], and the data are given in Table 1.

Table 1 Thermal properties

Sl. no	Sample	T_g (°C)	T_m (°C)	ΔH_m (J g^{-1})	x_c (%)
1	PEO	−65.12	69	153.37	71.76
2	PEO-PVDF	−67.55	67	122.6	57.37
3	PEO-PVDF-$LiNO_3$ 12 weight%	−73.88	66	25.87	12.10
4	PEO-PVDF-$LiNO_3$ 12 weight%-Al_2O_3 2 weight%	−76.47	66	20.86	9.76

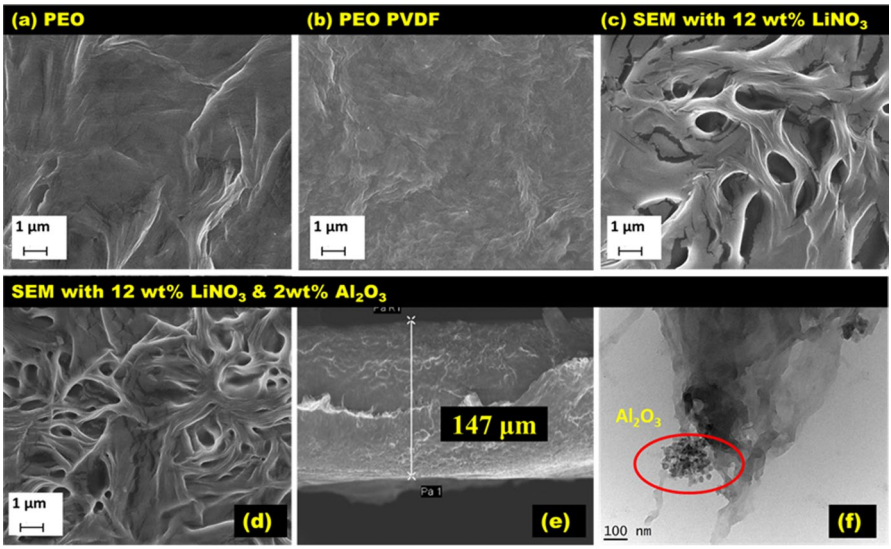

Fig. 6 FESEM images of **a** PEO, **b** PEO-PVDF polymer blend, **c** SEM with 12 weight% of $LiNO_3$, and **d** SEM with 12 weight% of $LiNO_3$ and 2 weight% of Al_2O_3 **e** cross sectional view of SEM with 12 weight% of $LiNO_3$ and 2 weight% of Al_2O_3 and **f** TEM image of SEM with 12 weight% of $LiNO_3$ and 2 weight% of Al_2O_3

Morphological studies

FESEM and TEM results constitute some of the highlights of the present work. FESEM micrographs of pure PEO, PEO-PVDF, PEO-PVDF-12 weight% $LiNO_3$, PEO-PVDF-12 weight% $LiNO_3$-2 weight% Al_2O_3 and TEM image of PEO-PVDF-12 weight% $LiNO_3$-2 weight% Al_2O_3 are shown in Fig. 6. Due to the rigid nature of PEO, several micro-cracks and craters are seen on its rough microstructure, as shown in Fig. 6a. which may be due to the rapid and uneven evaporation of DMF solvent during the drying process of the polymer blend electrolyte. After the blend formation of PEO with PVDF, the micro-cracks disappear, and the polymer blend surface becomes smoother and more flexible [45], as shown in Fig. 6b. On the addition of lithium salt (Fig. 6c), several micro-pores are formed on the surface of the resulting SE membrane, and the smooth appearance of the blend is retained.

On adding filler Al_2O_3, more micro-pores are additionally formed, and they are homogeneously distributed, resulting in increased surface areas seen from Fig. 6d. Enhanced surface area grants more pathways for ion transport with low activation energy which is favorable for ion conduction [47]. These micro-pores have an average size of around 1.5 μm. The membrane thickness is 147 μm from the cross-sectional FESEM image shown in Fig. 6e. No phase separation is visible in this micrograph, suggesting the possibility of rapid transport of ions without any blocking phase. PEO-PVDF polymer network and Al_2O_3 nanoparticles embedded in the polymer blend are visible in the TEM image, shown in Fig. 6f. Presence of 2 weight% Al_2O_3 nanofiller in PEO-PVDF-12 weight% $LiNO_3$ polymer blend complex induces a topological disorder which improves the porosity and flexibility of the SE membrane. Consequently, room temperature ionic conductivity also gets enhanced due to the easy penetration of Li ions through the porous structure [48].

Electrochemical studies

The ionic conductivity of SE membranes is determined from electrochemical impedance studies conducted by sandwiching them between two stainless steel disks which act as blocking electrodes for Li ions under an applied electric field. Impedance plots of the PEO-PVDF blend system complexed with different weight percentages of $LiNO_3$ and Al_2O_3 are shown in Fig. 7a and b. The resulting Nyquist plots contain high-frequency semi-circular and low-frequency straight-line regions related to ionic conduction and the effect of blocking electrodes, respectively. The capacitive interface forming an intercept at the high-frequency side of the Z_i axis gives bulk resistance R_b [49]. Room temperature ionic conductivity (σ) of various samples is calculated using Eq. (1) and tabulated in Table 2:

$$\sigma = \frac{t}{R_b A} \tag{1}$$

where t and A are the thickness and area of the membrane, respectively.

Adding Li salt to the PEO- PVDF polymer blend results in an increase in carrier ion concentration and leads to enhancement in ionic conductivity. The maximum ionic conductivity observed is 3.01×10^{-5} S cm^{-1} for the membrane with 12 weight% of $LiNO_3$ in the PEO-PVDF polymer blend. Further addition of Li salt decreases ionic conductivity due to the aggregation of ions in the polymer blend matrix, and the agglomerates act as blocks against free ion motion. Also, the anion $(NO_3)^-$, which inhibits restacking of polymer segments, causes retention of the amorphous phase down to ambient temperatures. One of the significant outcomes of the present work is the positive influence of the filler Al_2O_3 on the structural and electrochemical characteristics of the SE membranes. There is a substantial increase in ionic conductivity with the addition of filler Al_2O_3, and the maximum ionic conductivity observed is 1.25×10^{-4} S cm^{-1} for the SE membrane containing 2 weight% Al_2O_3. The larger surface area of nanostructured ceramic filler hinders local PEO chain rearrangement, resulting in amorphous phase locking, which favors enhanced

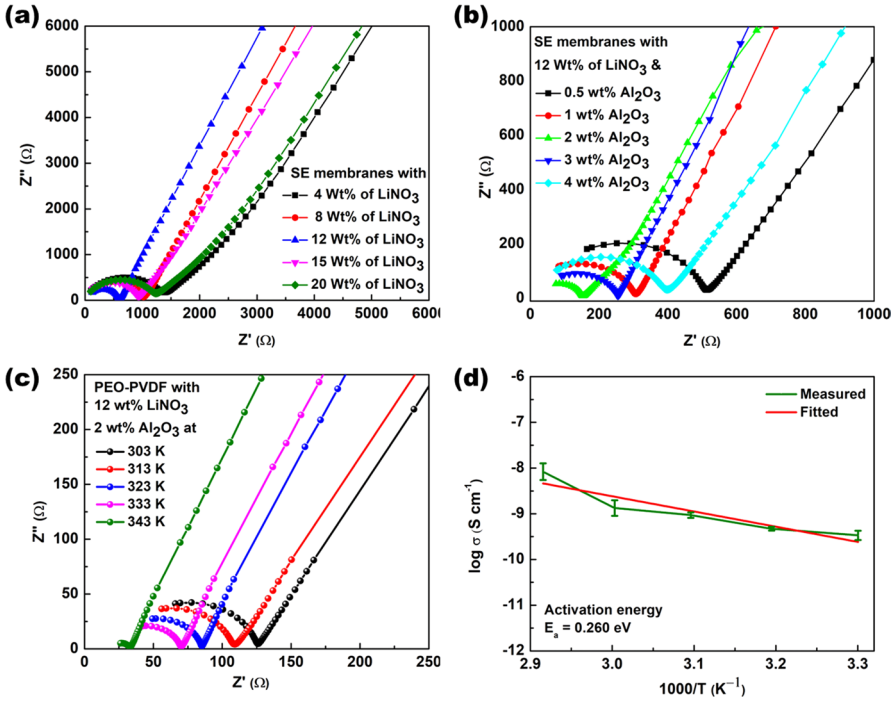

Fig. 7 EIS spectra of **a** SE membranes with different weight% of $LiNO_3$ **b** SE membranes with 12 weight% of $LiNO_3$, and different weight% of Al_2O_3 0.5, 1, 2, 3, and 4 **c** Temperature variation of SE membrane with 12 weight% of $LiNO_3$, and 2 weight% of Al_2O_3 and **d** Arrhenius plot of SE membrane with 12 weight% of $LiNO_3$, and 2 weight% of Al_2O_3

Table 2 Ionic conductivity of solid electrolyte membranes with different weight% of Al_2O_3 nanofiller

Sl. no	Solid electrolyte membrane	Bulk resistance/R_b (Ω)	Ionic conductivity/ σ (S cm^{-1})
1	PEO-PVDF-$LiNO_3$ 12 weight%- Al_2O_3 0.5 weight%	517	$3.61*10^{-5}$
2	PEO-PVDF-$LiNO_3$ 12 weight%- Al_2O_3 1 weight%	311	$6.01*10^{-5}$
3	PEO-PVDF-$LiNO_3$ 12 weight%- Al_2O_3 2 weight%	149	$1.25*10^{-4}$
4	PEO-PVDF-$LiNO_3$ 12 weight%- Al_2O_3 3 weight%	252	$7.41*10^{-5}$
5	PEO-PVDF-$LiNO_3$ 12 weight%- Al_2O_3 4 weight%	397	$4.70*10^{-5}$

ionic transport [50]. Ionic conductivity increases initially to reach the maximum value and then decreases on further addition of filler due to the blocking effect imposed by more abundant alumina grains. The variation of ionic conductivity with filler is shown in Table 2.

Ionic conductivity is achieved by creating crosslinking centers for PEO segments and anions, by lowering PEO reorganizing tendency and retaining the amorphous phase down to ambient temperatures, by promoting Li^+ ion conducting pathways

at the ceramic surface [51], and by forming Lewis acid/base centers with ionic species, resulting in ionic dissociation and the formation of additional cations [52]. For diverse polymer blends, the effect of Al_2O_3nanofiller on improving ionic conductivity has already been described. In general, nano-sized alumina grains help to increase ionic conductivity in different ways [53–55]. Nyquist plots (Fig. 7c) and Arrhenius plot (Fig. 7d) show the variation of ionic conductivity with temperature in the 303–343 *K* range of the finally optimized SE membrane. Ionic conductivity increases with an increase in temperature due to polymer expansion producing free volume, which facilitates enhancement in both inter-polymer segmental and ionic mobility, which in turn gives rise to an increase in ionic conductivity [56]. Plots of logs of ionic conductivity versus temperature follow the Arrhenius behavior throughout the temperature range. Variation of ionic conductivity (σ) with temperature (*T*) can be fitted to Arrhenius equation given as follows [57]:

$$\sigma = \sigma_0 \exp\left(\frac{-E_a}{kT}\right) \tag{2}$$

The slope of the Arrhenius plot is used to calculate the thermal activation energy E_a of the SE membrane, which is found to be 0.26 eV. It is the energy required to create a proper conductive environment for the ions to migrate smoothly and efficiently through the polymer matrix.

Cyclic voltammetry response of the finally optimized SE membrane (PEO-PVDF-12 weight% of $LiNO_3$- 2 weight% of Al_2O_3) (SS//SEM//SS) was studied, and the CV curves (initial 4 cycles) are shown in Fig. 8a. Four cycles of CV curves do not offer any distinct peaks anywhere, which indicates the purity, reproducibility, and electrochemical stability of the optimized SE membrane. From the CV curve, the stability window of the optimized SE membrane is found to be in the voltage range of 0 to 4 V, which makes these SE membranes highly promising for high-voltage cell applications. Electrochemical stability of the optimized solid polymer electrolyte (SE) membrane was assessed using linear sweep voltammetry technique at a scan rate of 5 mV s^{-1} within the potential window of 0 to 6 V (versus Li/Li.$^+$), using the configuration of SS//SE//Li and the LSV curve is shown in Fig. 8b. A rapid increase in current at around 4.75 V is observed, indicating anodic breakdown of the membrane due to the decomposition of the SE. It is concluded that our optimized membrane is stable up to 4.75 V and can safely operate in combination with high-voltage cathode materials without undergoing electrochemical oxidative decompositions [58].

Wagner's DC polarization technique is a basic method to calculate the total ionic transport number. It has been carried out by applying 0.5 V across SS// SE//SS configuration (where SS stands for stainless steel).Then, the cell develops a direct current as a function of time. The total ion transport number t_{ion} is calculated using the plot of current variation with time for the optimized SE membrane and is given in Fig. 8c. The value obtained is 0.999, which is very close to the theoretical value of unity. It is evident that the conductivity of the SE membranes is mainly ionic, and electron contribution is negligible.

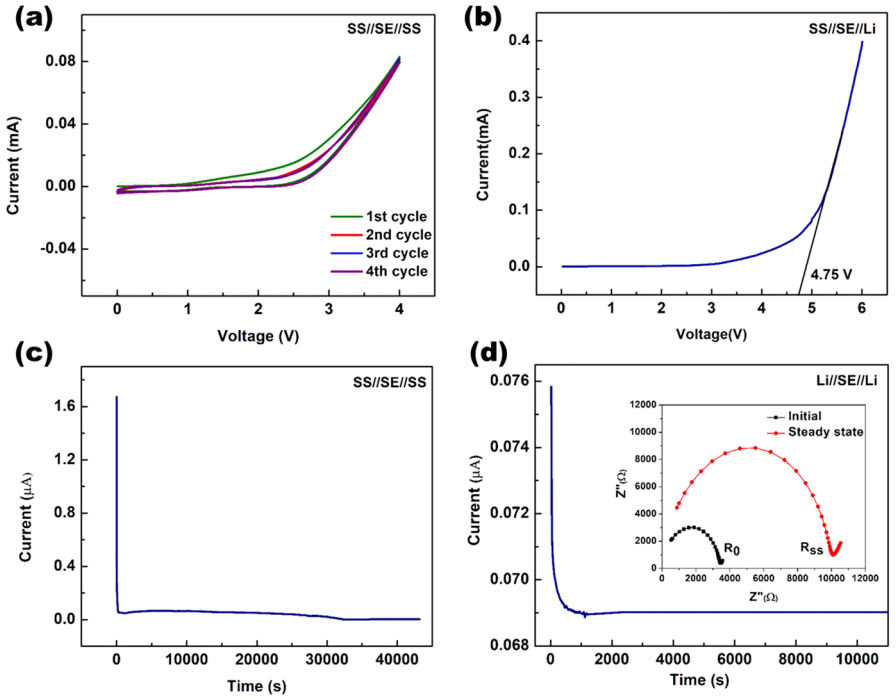

Fig. 8 **a** Cyclic voltammetry curves (initial 4 cycles) **b** Linear sweep voltammetry curve **c** Transport number studies curve and **d** Transference number studies curve (inset Nyquist plot) of SE membrane with 12 weight% of $LiNO_3$and 2 weight% of Al_2O_3

Evans and Vincent's method has been used to find lithium-ion transference numbers (T_{Li}). On applying a potential of 1 V to the assembled symmetric cell with the configuration, Li//SE//Li, the initial current through the cell is found to decrease with time until a steady-state value (*I*ss) [59] is obtained, as shown in Fig. 8d and the corresponding EIS spectra of the cell during the initial and steady state are shown as inset. The decrease in current is due to the formation of the carrier concentration gradient across the cell. The number of active charge carriers decreases, and as a result, the current also decreases. Lithium-ions are the only charge-carrying species in the steady state and contribute toward the steady-state current [60]. Lithium-ion transference number obtained is 0.33. Lewis acid–base interaction between Al_2O_3 and PEO-PVDF- $LiNO_3$ complex electrolyte can inhibit interactions between $(NO_3)^-$ anion and Li^+ cation, creating more free Li^+ ions. In the present study, Al_2O_3 has a Lewis acid center that can interact with the anions of $LiNO_3$ salt, and these interactions reduce the crystallinity of the polymer host. This reduction in crystallinity could be the reason for enhanced ion transportation [61]. The presence of filler material can reduce electrode polarization induced by anion buildup and attenuate the concentration gradient by

reducing dendrite formation and thus facilitate high lithium-ion transport. Even though this number is lower than the anionic transference number of 0.67, the former ensures that Li^+ ions move between the electrodes [62–64].

Li-ion cell assembling and testing

$LiFePO_4$ (LFP) is rated as a very attractive cathode material due to its high theoretical specific capacity (170 mAh g^{-1}), good thermal stability, low cost, and environmental friendliness [65]. Prototype, fully solid-state Li-ion cells were assembled with SE membrane with 12 weight% of $LiNO_3$ and 2 weight% of Al_2O_3 (SEM) acting as both solid electrolyte and separator and using LFP-multiwalled carbon nanotubes (MWCNT) nanocomposite as a cathode in half-cell configuration (Li/ Li^+// SEM//LFP-MWCNT) and cell performance was tested by cyclic voltammetry(CV) and galvanostatic charge–discharge (GCD) studies. CV and GCD curves of the initial cycles are shown in Fig. 9a and b, respectively. Charge–discharge cycling for 100 cycles has been carried out at 70 ℃ at a current rate of C/10 (Fig. 10a). The voltage plateau of the cells remains almost steady during cycling, indicating that the polarization of the system is very weak [66]. Expected flat plateaus centered at 3.45 V are seen in the curves, reflecting the two-phase electrochemical reaction of the LFP active material as shown below in Eq. (3).

$$\mathrm{LiFePO_4} \leftrightarrow Li^+ + e^- + \mathrm{FePO_4} \tag{3}$$

A photograph of assembled cell showing an open circuit voltage of 3.44 V is depicted in Fig. 10b. Cells deliver an initial charge capacity of 125 mAh g^{-1} and an initial discharge capacity of 128 mAh g^{-1}. After a few cycles, the cells attain a stable electrode–electrolyte interface (EEI), and then, a small capacity fading occurs on further cycling. The charge capacity falls to 100 mAh g^{-1} and the discharge capacity to 108mAh g^{-1} with a capacity retention of 84% after 100 cycles. For LFP material, capacity reduction at a higher current rate is typically observed. The observed stability loss can be related to the following aspects of the fully solid-state cells

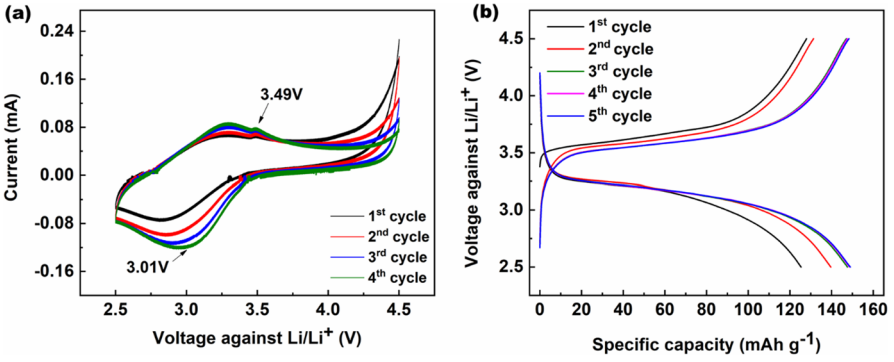

Fig. 9 **a** CV curves (initial 4 cycles) at 0.1mVs^{-1} and **b** GCD curves (initial 5 cycles) at 0.1 C of Li/Li^+// SEM//LFP-MWCNT half-cell

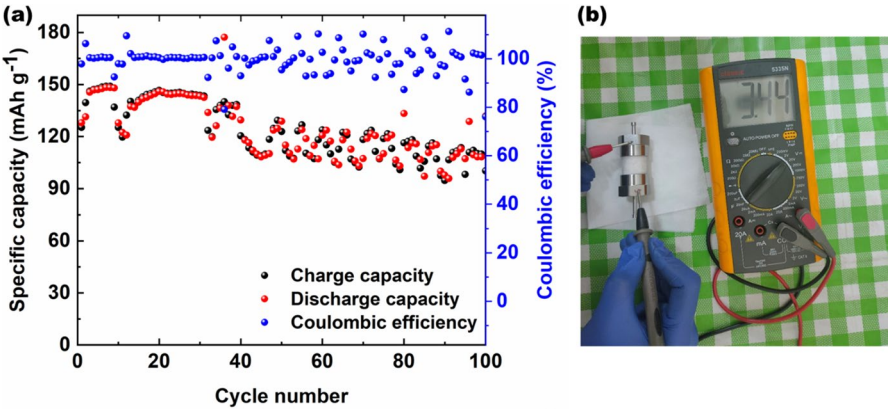

Fig. 10 **a** Cycling stability curve of LFP-MWCNT electrode in Li/Li$^+$// SEM//LFP-MWCNT (100 cycles at 0.1 C) and **b** photograph of assembled Swagelok-type cell showing open circuit voltage of 3.44 V

assembled in the present work. Successive generation and growth of lithium dendrites on the anode dilute the contact between the electrode and solid electrolyte membrane, increasing anode resistance. Accumulated decomposition products will gradually increase the reaction resistance of the cathode [67]. Despite the observed capacity decay with cycling, present results on the working of the fully solid-state Li-ion cells assembled using the developed SE membranes are promising and offer ample scope for further investigations to rectify the drawbacks and thus improve cell performance.

Post-mortem studies

Aged Li-ion cells (Li/Li$^+$//SEM//LFP-MWCNT) were investigated after being subjected to 100 charge–discharge cycles at 0.1 C using post-mortem analysis. The test cell was allowed to discharge to the end of discharge voltage and was disassembled in chemically inert atmosphere inside an argon-filled glove box with humidity less than 5 ppm. After separating the components, electrodes, and SE membranes, the LFP-MWCNT cathode was washed with DMC (dimethyl carbonate) for 2 min, dried at 50 ℃ inside Ar filled glove box, and subjected to morphological studies [68]. The FESEM images of the LFP-MWCNT cathode before and after cycling (100 cycles at 0.1 C) are shown in Fig. 11a and b, respectively. From the FESEM images, the particle size of LFP-MWCNT cathode material has been calculated as 120–150 nm. Volume expansion and pulverization of cathode active material upon cycling can be observed in the FESEM image, consequent to post-mortem analysis, constituting the significant factors for capacity fading. Capacity decay of the cell is mainly due to an unstable EEI layer, volume expansion, cracking and pulverization, and loss of electrical contacts.

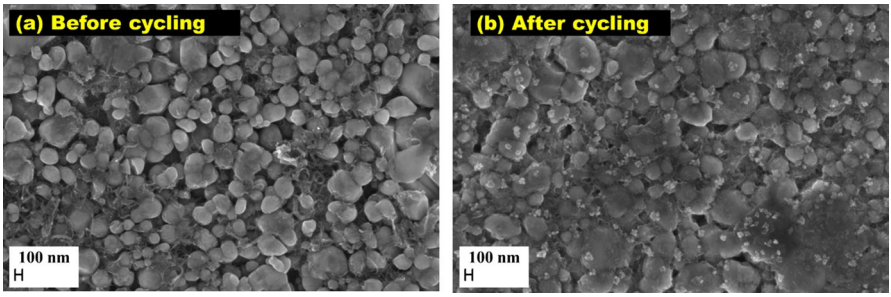

Fig. 11 FESEM images of LFP-MWCNT electrode **a** before cycling and **b** after 100 cycles at 0.1 C

Conclusions

Developing stable, safe, and efficient solid-state electrolytes in flexible and free-standing form is beneficial for realizing fully solid-state lithium-ion cells with commendable performance efficiency. The present work focuses on strategies to enhance the lithium-ion conductivity of solid polymer electrolyte membranes developed using the polymer blend of PEO and PVDF, complexed with $LiNO_3$ as lithium source and enriched with ceramic nanofiller Al_2O_3. Freestanding, flexible, and transparent SE membranes grown for the combination, PEO-PVDF-12 weight% of $LiNO_3$-2 weight% of Al_2O_3 are found to show enhanced room temperature ionic conductivity around 1.25×10^{-4} S cm^{-1}, with electrochemical stability up to 4.75 V, and thermal stability up to 430 ℃. Reduced crystallinity and enhancement in the amorphous nature of the polymer blend on treatment with lithium salt and further enhancement in the amorphous, flexible, and porous nature of the resulting SE on enriching with an optimized concentration of Al_2O_3 are the prime factors contributing towards enhanced ionic conductivity and good electrochemical stability of the SE membranes. Creation of favorable conducting pathways through Lewis acid–base type interactions of ionic species with O/OH surface groups on alumina nanofiller grains is also instrumental in the enhancement of ionic conductivity. Assembled fully solid-state Li/ Li^+//SEM// LFP-MWCNT cell exhibits good cell performance with initial charge–discharge capacity of 125 mAh g^{-1} and 128 mAh g^{-1}, respectively, at a current rate of 0.1 C at 70 ℃. Choice of suitable combinations of host polymers, plasticizers, lithium salts and nanofillers for achieving stable EEI upon cycling is a viable option for improving the performance of fully solid-state Li ion cells.

Acknowledgements One of the authors, Merin K. Wilson, thanks Rashtriya Uchchatar Shiksha Abhiyan (RUSA), Government of India, for financial support through senior research fellowship. The authors acknowledge the funding extended by the Department of Science and Technology, Government of India, in the form of the Funding for Improvement of Science and Technology (DST-FIST) Scheme, for acquiring FE- SEM facility. The authors also acknowledge STIC, CUSAT, Kerala, India, for TEM, DSC, and TGA measurements. S. Jayalekshmi is thankful for the financial assistance from Kerala State Council for Science, Technology, and Environment (KSCSTE) via Emeritus Scientist Scheme.

Declarations

Conflict of interest The authors declare that they have no conflict of interest.

References

1. Goodenough JB, Park KS (2013) The Li-ion rechargeable battery: a perspective. J Am Chem Soc 135(4):1167–1176. https://doi.org/10.1021/ja3091438
2. Tarascon JM, Armand M (2010) Issues and challenges facing rechargeable lithium batteries. Mater Sustain Energy Collect Peer-Rev Res Rev Artic Nat Publ Gr 414:171–179. https://doi.org/10.1142/9789814317665_0024
3. Yang H, Zhuang GV, Ross PN (2006) Thermal stability of LiPF6 salt and Li-ion battery electrolytes containing LiPF6. J Power Sources 161(1):573–579. https://doi.org/10.1016/j.jpowsour.2006.03.058
4. Aurbach D (2000) Review of selected electrode-solution interactions which determine the performance of Li and Li-ion batteries. J Power Sour 89(2):206–218. https://doi.org/10.1016/S0378-7753(00)00431-6
5. Ahmad S (2009) Polymer electrolytes : characteristics and peculiarities. Ionics 15:309–321. https://doi.org/10.1007/s11581-008-0309-x
6. Wu F, Feng T, Bai Y, Wu C, Ye L, Feng Z (2009) Preparation and characterization of solid polymer electrolytes based on PHEMO and PVDF-HFP. Solid State Ionics 180(9–10):677–680. https://doi.org/10.1016/j.ssi.2009.03.003
7. Kumar KN, Kang M, Sivaiah K, Ravi M, Ratnakaram YC (2016) Enhanced electrical properties of polyethylene oxide (PEO) + polyvinylpyrrolidone (PVP):Li+ blended polymer electrolyte films with the addition of Ag nanofiller. Ionics (Kiel) 22(6):815–825. https://doi.org/10.1007/s11581-015-1599-4
8. Pradeepa P, Edwin Raj S, Sowmya G, Kalaiselvimary J, Ramesh Prabhu M (2016) Optimization of hybrid polymer electrolytes with the effect of lithium salt concentration in PEO/PVdF-HFP blends. Mater Sci Eng B Solid-State Mater Adv Technol 205:6–17. https://doi.org/10.1016/j.mseb.2015.11.009
9. Croce F, Curini R, Martinelli A, Persi L, Ronci F, Scrosati B, Caminiti R (1999) Physical and chemical properties of nanocomposite polymer electrolytes. J Phys Chem B 103(48):10632–10638. https://doi.org/10.1021/jp992307u
10. Weston JE, Steele BCH (1982) Effects of inert fillers on the mechanical and electrochemical properties of lithium salt-poly(ethylene oxide) polymer electrolytes. Solid State Ionics 7(1):75–79. https://doi.org/10.1016/0167-2738(82)90072-8
11. Links DA (2011) Electrolytes for solid-state lithium rechargeable batteries : recent advances and perspectives. Chem Soc Rev. https://doi.org/10.1039/c0cs00081g
12. Zhang XW, Wang C, Appleby AJ, Little FE (2002) Characteristics of lithium-ion-conducting composite polymer-glass secondary cell electrolytes. J Power Sources 112(1):209–215. https://doi.org/10.1016/S0378-7753(02)00365-8
13. Appetecchi G, Croce F, Hassoun J, Scrosati B, Salomon M, Cassel F (2003) Hot-pressed, dry, composite, PEO-based electrolyte membranes: I. Ionic conductivity characterization. J Power Sources 114:105–112. https://doi.org/10.1016/S0378-7753(02)00543-8
14. Liang B, Liang B, Tang S, Jiang Q, Chuangsheng Chen Xu, Chen SL, Yan X (2015) Preparation and characterization of PEO-PMMA polymer composite electrolytes doped with nano-Al2O3. Electrochim Acta 169:334–341. https://doi.org/10.1016/j.electacta.2015.04.039
15. Kesavan K, Mathew CM, Rajendran S (2014) Lithium ion conduction and ion-polymer interaction in poly(vinyl pyrrolidone) based electrolytes blended with different plasticizers. Chinese Chem Lett 25(11):1428–1434. https://doi.org/10.1016/j.cclet.2014.06.005
16. El Achaby M, Arrakhiz FZ, Vaudreuil S, Essassi EM, Qaiss A (2012) Piezoelectric [illegible] -polymorph formation and properties enhancement in graphene oxide – PVDF nanocomposite films. Appl Surf Sci 258(19):7668–7677. https://doi.org/10.1016/j.apsusc.2012.04.118
17. Jacob MME, Prabaharan SRS, Radhakrishna S (1997) Effect of PEO addition on the electrolytic and thermal properties of PVDF-LiClO4 polymer electrolytes. Solid State Ionics 104(3–4):267–276. https://doi.org/10.1016/s0167-2738(97)00422-0

18. Shan Y, Li L, Yang X (2021) Solid-state polymer electrolyte solves the transfer of lithium ions between the solid-solid interface of the electrode and the electrolyte in Lithium-Sulfur and Lithium-ion batteries. ACS Appl Energy Mater 4(5):5101–5112. https://doi.org/10.1021/acsaem.1c00658
19. Judeinstein BP, Roussel F (2005) Ionic conductivity of lithium salt/Oligo ethylene oxide based liquid-crystal mixtures : the effect of molecular architecture on the conduction process. Adv Mater 6:723–727
20. Jinisha B, Anilkumar KM, Manoj M, Pradeep VS, Jayalekshmi SJEA (2017) Development of a novel type of solid polymer electrolyte for solid state lithium battery applications based on lithium enriched poly (ethylene oxide)(PEO)/poly (vinyl pyrrolidone)(PVP) blend polymer. Electrochim Acta 235:210–222. https://doi.org/10.1016/j.electacta.2017.03.118
21. Hou W, Zhai Y, Chen Z, Liu C, Ouyang C, Hu N, Song S (2023) Fluorine-regulated cathode electrolyte interphase enables high-energy quasi-solid-state lithium metal batteries. Appl Phys Lett 10(1063/5):0134474
22. Yang G, Hou W, Zhai Y, Chen Z, Liu C, Ouyang C, Song S (2023) Polymeric concentrated electrolyte enables simultaneous stabilization of electrode/electrolyte interphases for quasi-solid-state lithium metal batteries. EcoMat. https://doi.org/10.1002/eom2.12325
23. Li C, Zhou S, Dai L, Zhou X, Zhang B, Chen L, Zeng T, Liu Y, Tang Y, Jiang J, Huang J (2021) Porous polyamine/PEO composite solid electrolyte for high-performance solid-state lithium metal batteries. J Mater Chem A 9(43):24661–24669. https://doi.org/10.1039/d1ta04599g
24. Long L, Wang S, Xiao M, Meng Y (2016) Polymer electrolytes for lithium polymer batteries. J Mater Chem A 4(26):10038–10039. https://doi.org/10.1039/c6ta02621d
25. Tominaga Y, Endo M (2013) Ion-conductive properties of polyether-based composite electrolytes filled with mesoporous silica, alumina, and titania. Electrochim Acta 113:361–365. https://doi.org/10.1016/j.electacta.2013.09.117
26. Mohamed Ali T, Padmanathan N, Selladurai S (2015) Effect of nanofiller CeO_2 on structural, conductivity, and dielectric behaviors of plasticized blend nanocomposite polymer electrolyte. Ionics 21:829–840. https://doi.org/10.1007/s11581-014-1240-y
27. Ravi M, Kumar KK, Mohan VM, Rao VN (2014) Effect of nano TiO_2 filler on the structural and electrical properties of PVP based polymer electrolyte films. Polym Test 33:152–160. https://doi.org/10.1016/j.polymertesting.2013.12.002
28. Kou Y, Zhou W, Li X, Wang Z, Li Y, Cai H, Dang ZM (2020) Enhanced dielectric properties of PVDF nanocomposites with modified sandwich-like GO@ PVP hybrids. Polym Plast Technol Mater 59(6):592–605. https://doi.org/10.1080/25740881.2019.1669655
29. Jinisha B, Anilkumar KM, Manoj M, Abhilash A, Pradeep VS, Jayalekshmi S (2018) Poly (ethylene oxide) (PEO)-based, sodium ion-conducting, solid polymer electrolyte films, dispersed with Al_2O_3 filler, for applications in sodium ion cells. Ionics (Kiel) 24(6):1675–1683. https://doi.org/10.1007/s11581-017-2332-2
30. Croce F, Appetecchi GB, Persi L, Scrosati B (1998) Nanocomposite polymer electrolytes for lithium batteries. Nat Lett 394:456–458. https://doi.org/10.1038/28818
31. Gouda OE, Mahmoud SF, El-Gendy AA, Haiba AS (2014) Improving the dielectric properties of high density polyethylene by incorporating clay-nano filler. TELKOMNIKA Indonesian J Electr Eng 12(12):7987–7995. https://doi.org/10.12928/TELKOMNIKA.v12i4.115
32. Jayathilaka PARD, Dissanayake MAKL, Albinsson I, Mellander BE (2002) Effect of nano-porous Al2O3 on thermal, dielectric and transport properties of the (PEO)9LiTFSI polymer electrolyte system. Electrochim Acta 47(20):3257–3268. https://doi.org/10.1016/S0013-4686(02)00243-8
33. Bruce PG, Evans J, Vincent CA (1988) Conductivity and transference number measurements on polymer electrolytes. Solid State Ionics 28:918–922. https://doi.org/10.1016/0167-2738(88)90304-9
34. Christodoulou K, Andrikopoulos KS, Fotiadou S, Bollas S, Karageorgaki C, Dimitrios C, Voyiatzis GA, Anastasiadis SH (2011) Crystallinity and chain conformation in PEO/layered silicate nanocomposites. Macromolecules 44(24):9710–9722. https://doi.org/10.1021/ma201711r
35. Chauhan AK, Mishra K, Kumar D, Singh A (2021) Enhancing Sodium ion transport in a PEO-based solid polymer electrolyte system with $NaAlO_2$ active fillers. J Electron Mater 50(9):5122–5133. https://doi.org/10.1007/s11664-021-09051-y
36. Yi M, Wu X (2020) Dynamics of charged particles around a magnetically deformed Schwarzschild black hole. Phys Scr 95(8):085008. https://doi.org/10.1088/1402-4896/aba4c2
37. Li XH, Zhao LJ, Dong JL, Xiao HS, Zhang YH (2008) Confocal raman studies of Mg(NO3)2 aerosol particles deposited on a quartz substrate: supersaturated structures and complicated phase transitions. J Phys Chem B 112(16):5032–5038. https://doi.org/10.1021/jp709938x

38. Elashmawi IS, Gaabour LH (2015) Raman, morphology and electrical behavior of nanocomposites based on PEO/PVDF with multi-walled carbon nanotubes. Results Phys 5:105–110. https://doi.org/10.1016/j.rinp.2015.04.005
39. Kumar KN, Reddy MV, Vijayalakshmi L, Ratnakaram YC (2015) Synthesis and analysis of Fe_3+, Co_2+, and Ni_2+: PEO+ PVP blended polymer composite films for multifunctional polymer applications. Bull Mater Sci 38(4):1015–1023. https://doi.org/10.1007/s12034-015-0925-9
40. Puthirath AB, John B, Gouri C, Jayalekshmi S (2015) Lithium-doped PEO-a prospective solid electrolyte with high ionic conductivity, developed using *n*-Butyllithium in hexane as dopant. Ionics (Kiel) 21(8):2185–2191. https://doi.org/10.1007/s11581-015-1406-2
41. Kesavan K, Mathew CM, Rajendran S, Ulaganathan M (2014) Preparation and characterization of novel solid polymer blend electrolytes based on poly (vinyl pyrrolidone) with various concentrations of lithium perchlorate. Mater Sci Eng: B 184:26–33. https://doi.org/10.1016/j.mseb.2014.01.009
42. Rathika R, Padmaraj O, Suthanthiraraj SA (2018) Electrical conductivity and dielectric relaxation behavior of PEO/PVdF-based solid polymer blend electrolytes for zinc battery applications. Ionics (Kiel) 24(1):243–255. https://doi.org/10.1007/s11581-017-2175-x
43. Ganesan S, Muthuraaman B, Mathew V, Vadivel MK, Maruthamuthu P, Ashokkumar M, Suthanthiraraj SA (2011) Influence of 2, 6 (N-pyrazolyl) isonicotinic acid on the photovoltaic properties of a dye-sensitized solar cell fabricated using poly (vinylidene fluoride) blended with poly (ethylene oxide) polymer electrolyte. Electrochim Acta 56(24):8811–8817. https://doi.org/10.1016/j.electacta.2011.07.081
44. Sulaiman M, Rahman AA, Mohamed NS (2017) Effect of water-based sol-gel method on structural, thermal and conductivity properties of $LiNO_3$ – Al_2O_3 composite solid electrolytes. Arab J Chem 10(8):1147–1152. https://doi.org/10.1016/j.arabjc.2015.04.031
45. Choudhary S, Sengwa RJ (2017) Effects of different inorganic nanoparticles on the structural, dielectric and ion transportation properties of polymers blend based nanocomposite solid polymer electrolytes. Electrochim Acta 247:924–941. https://doi.org/10.1016/j.electacta.2017.07.051
46. Braun PV, Cho J, Pikul JH, King WP, Zhang H (2012) High power rechargeable batteries. Curr Opin Solid State Mater Sci 16(4):186–198. https://doi.org/10.1016/j.cossms.2012.05.002
47. Liu J, Khanam Z, Muchakayala R, Song S (2020) Fabrication and characterization of Zn-ion-conducting solid polymer electrolyte films based on PVdF-HFP/Zn(Tf)2 complex system. J Mater Sci Mater Electron 31(8):6160–6173. https://doi.org/10.1007/s10854-020-03169-1
48. Anilkumar KM, Jinisha B, Manoj M, Jayalekshmi S (2017) Poly(ethylene oxide) (PEO) – Poly(vinyl pyrrolidone) (PVP) blend polymer-based solid electrolyte membranes for developing solid-state magnesium ion cells. Eur Polym J 89:249–262. https://doi.org/10.1016/j.eurpolymj.2017.02.004
49. Michael MS, Jacob MME, Prabaharan SRS, Radhakrishna S (1997) Enhanced lithium ion transport in PEO-based solid polymer electrolytes employing a novel class of plasticizers. Solid State Ionics 98(3–4):167–174. https://doi.org/10.1016/s0167-2738(97)00117-3
50. Aravindan V, Vickraman P (2007) A novel gel electrolyte with lithium difluoro(oxalate)borate salt and Sb2O3 nanoparticles for lithium-ion batteries. Solid State Sci 9(11):1069–1073. https://doi.org/10.1016/j.solidstatesciences.2007.07.011
51. Singh R, Kumar J, Singh RK, Rastogi RC, Kumar V (2007) Low-frequency ac conduction and dielectric relaxation in pristine poly(3-octyl thiophene) films. New J Phys 9(3):227–232. https://doi.org/10.1088/1367-2630/9/2/040
52. Yakuphanoglu F, Aydogdu Y, Schatzschneider U, Rentschler E (2003) DC and AC conductivity and dielectric properties of the metal-radical compound: Aqua [bis(2-dimethylaminomethyl-4-NIT-phenolato)]copper(II). Solid State Commun 128(2–3):63–67. https://doi.org/10.1016/S0038-1098(03)00651-3
53. Chapi S, Raghu S, Devendrappa H (2016) Enhanced electrochemical, structural, optical, thermal stability and ionic conductivity of (PEO/PVP) polymer blend electrolyte for electrochemical applications. Ionics 22(6):803–814. https://doi.org/10.1007/s11581-015-1600-2
54. Chen D, Cheng J, Wen Y, Cao G, Yang Y, Liu H (2012) Impedance study of electrochemical stability limits for electrolytes. Int J Electrochem Sci 7:12383–12390. https://doi.org/10.1016/S1452-3981(23)16552-7
55. Kumar KK, Pavani Y, Ravi M, Bhavani S, Sharma AK, Rao VVRN (2011) Effect of complexation of NaCl salt with polymer blend (PEO/PVP) electrolytes on ionic conductivity and optical energy band gaps. AIP Conf Proc 1391:641–644. https://doi.org/10.1063/1.3643635

56. Zugmann S, Fleischmann M, Amereller M, Gschwind RM, Wiemhöfer HD, Gores HJ (2011) Measurement of transference numbers for lithium-ion electrolytes via four different methods, a comparative study. Electrochim Acta 56(11):3926–3933. https://doi.org/10.1016/j.electacta.2011.02.025
57. Zhang H, Liu C, Zheng L, Fei Xu, Feng W, Li H, Huang X, Armand M, Nie J, Zhou Z (2014) Lithium bis(fluoro sulfonyl)imide/poly(ethylene oxide) polymer electrolyte. Electrochim Acta 133:529–538. https://doi.org/10.1016/j.electacta.2014.04.099
58. Dissanayake MAKL, Jayathilaka PARD, Bokalawala RSP, Albinsson I, Mellander BE (2003) Effect of concentration and grain size of alumina filler on the ionic conductivity enhancement of the (PEO)9LiCF$_3$SO$_3$:Al$_2$O$_3$ composite polymer electrolyte. J Power Sour 119–121:409–414. https://doi.org/10.1016/S0378-7753(03)00262-3
59. Kumar MS, Rao MC (2019) Effect of Al2O3 on structural and dielectric properties of PVP-CH3COONa based solid polymer electrolyte films for energy storage devices. Heliyon. https://doi.org/10.1016/j.heliyon.2019.e02727
60. Pitawala HMJC, Dissanayake MAKL, Seneviratne VA (2007) Combined effect of Al$_2$O$_3$ nano-fillers and EC plasticizer on ionic conductivity enhancement in the solid polymer electrolyte (PEO)9LiTf. Solid State Ionics 178(13–14):885–888. https://doi.org/10.1016/j.ssi.2007.04.008
61. Sengwa RJ, Dhatarwal P, Choudhary S (2014) Role of preparation methods on the structural and dielectric properties of plasticized polymer blend electrolytes: correlation between ionic conductivity and dielectric parameters. Electrochim Acta 142:359–370. https://doi.org/10.1016/j.electacta.2014.07.120
62. St-Onge V, Cui M, Rochon S, Daigle JC, Claverie JP (2021) Reducing crystallinity in solid polymer electrolytes for lithium-metal batteries via statistical copolymerization. Commun Mater 2(1):1–11. https://doi.org/10.1038/s43246-021-00187-2
63. Rosenwinkel MP, Schönhoff M (2019) Lithium transference numbers in PEO/LiTFSA electrolytes determined by electrophoretic NMR. J Electrochem Soc 166(10):A1977–A1983. https://doi.org/10.1149/2.0831910jes
64. Shao Y, Gudla H, Brandell D, Zhang C (2022) Transference number in polymer electrolytes: mind the reference-frame gap. J Am Chem Soc 144(17):7583–7587. https://doi.org/10.1021/jacs.2c02389
65. Ji G, Ou X, Zhao R, Zhang J, Zou J, Li P, He D (2021) Efficient utilization of scrapped LiFePO$_4$ battery for novel synthesis of Fe$_2$P$_2$O$_7$/C as candidate anode materials. Resour Conserv Recycl 174:105802. https://doi.org/10.1016/j.resconrec.2021.105802
66. Angulakshmi N, Kar GP, Bose S, Gowd EB, Thomas S, Stephan AM (2017) A high-performance BaTiO3-grafted-GO-laden poly(ethylene oxide)-based membrane as an electrolyte for all-solid lithium-batteries. Mater Chem Front 1(2):269–277. https://doi.org/10.1039/c6qm00098c
67. Appetecchi GB, Hassoun J, Scrosati B, Croce F, Cassel F, Salomon M (2003) Hot-pressed, solvent-free, nanocomposite, PEO-based electrolyte membranes: II All solid-state Li/LiFePO4 polymer batteries. J Power Sour 124(1):246–253. https://doi.org/10.1016/S0378-7753(03)00611-6
68. Waldmann T, Iturrondobeitia A, Kasper M, Ghanbari N, Aguesse F, Bekaert E, Wohlfahrt-Mehrens M (2016) Post-mortem analysis of aged lithium-ion batteries: disassembly methodology and physico-chemical analysis techniques. J Electrochem Soc 163(10):A2149. https://doi.org/10.1149/2.1211609jes

ISSN:2582-550X

'*Vinchi Pattukal'* A Diverse Cultural Representation of The Mappila *Khalasis* in Kerala

Nasreena P.K

The Khalsis played a significant role in the maritime history of Malabar, boasting a distinct identity for their unparalleled technical expertise in handling heavy goods. The origin of Khalasi is seen as a fusion of Arab and local indigenous groups, with the term Khalasi being derived from the Arabic word Khalasi which means black and white together. Khalasis remained relevant and adapted to the changing times by embracing modern technology and integrating it into their work. Despite the shift in job roles, their expertise in handling equipment and their skills were still highly valued. From the initial period, Khalasis played a vital role in the coastal areas of Beypore and gradually extended their settlements to other coastal areas like Chaliyam, Karuvanthuruthy, and Feroke, depending on the possibilities of their work. Their expertise in using these tools made their work much simpler and more efficient. Several traditional songs and chants associated with their heavy work are known as "Vinchipattukal" "Ambapattukal" and "Elayya pattukal," which signify their historical connection with their profession. The Panipattu or Vinchi pattukal were not limited to just artistic expressions; they served a greater purpose in creating a sense of unity and strength among the laborers. The chief purpose of the Khalasis using work songs is to gain energy and motivation for

their work. These songs provide a source of strength for the workers. These work songs, such as Amba pattukal, play a vital role in the Khalasi community, representing their culture, customs, and collective spirit. The songs serve as a reminder of their shared heritage and inspire unity among Khalasis making them an essential element of their cultural identity.

Key Words: Khalasis, Muppan, Vinchipattukal, Daver, Kappi, Ambapattukal, Elayyapattukal, Panipattu.

The *Khalasis*, played a significant role in the maritime history of Malabar. They had a distinct identity for their technical expertise in handling heavy goods. However, with changing times and the transformation of coastal areas, the significance of *Khalasi* community gradually faded from the mainstream maritime history of Malabar. Despite being a major social group in the Malabar coastal region, their role in Kerala's maritime history remained largely unexplored. This article tries to shed light on the significance of the social history of Malabar. The present study attempts to explore the uniqueness of *Khalasis* traditional work song, known as *vinchi pattukal*. When we look into the different aspects of *khalasi* work culture, definitely have to focus on their settlements. This article tries to analyse the historical significance of their coastal settlements. The primary objective of this paper is to preserve their legacy, highlighting their contributions to Kerala's cultural heritage, which has remained unnoticed.

Tracing the Roots: Historical Exploration of the Khalasi Community

The Arabs were the most significant contributors to the coastal trade and the cultural history of Kerala. Even before the rise of Islamic expansion, Arabs played a crucial role in commercial ties with Kerala. Both Kerala and Arabs share the centuries-old heritage of trade and cultural exchange. The great commercial relations between Kerala and the Arab world were one of the main reasons for the establishment of Arab settlements on the seashore of Kerala. The dynamic trading culture influenced the Malabar Coast to open up a new space for diverse religions. During the early period of Islamic emergence in Kerala, the construction of Muslim mosques showed architectural

similarities with Hindu temples, representing a level of assimilation of Hindu- Muslim community.

Arab traders came to Kerala's seashores to trade and cater to the needs of the large wooden boats. They were settled in various coastal regions of Malabar. During that time, they married local women, and this led to the formation of a new marriage tradition in Kerala. The marriage was known as *Mutha* marriage This custom of marriage was well-known in the region of Malabar. The *mutha* marriage was a conventional practice that was not comparable to any other custom prevalent at that time in Malabar. *Mutha* marriage was not considered regular marriages and did not involve customary rituals. Arab traders, who temporarily settled in the coastal regions with the intention of living there for a certain period to carry out their trade and fulfill their needs. So, the Arab traders engaged in *mutha* marriages. This kind of marriage had several distinctive features. As a result, a new generation was born with a mixed heritage of both Arab and local communities. The offspring born through this relationship are considered to have a mixed heritage, with both Arab and indigenous backgrounds. They are seen as a fusion of Arab and local groups known as *Khalasi*. The term *Khalasi* is derived from the Arabic word *Khilasiyy* which means black and white together. The word is reflecting the acknowledgment of the mixed heritage of the children born from these marriages (personal interview, Haasan Koya, 26th January, 2023).

Beypore was one of the most significant ports town in ancient Kerala. From the early period, *Khalasis* played a vital role in the coastal areas of Beypore. Gradually they extended their settlements to other coastal areas like Chaliyam, Karuvanthuruthy, and Ferok, depending on the possibilities of their work. Their technical skills, physical strength, and expertise in performing heavy physical tasks on both land and sea made them a vital part of different labor-intensive projects (C.P. Musthafa, 2019, 337). The technical skills possessed by *Khalasis* allowed them to tackle challenging tasks on both sea and land, along with their counterparts in other labor fields. They held a significant position in the labor sector during that period. However, as technology advanced, their exclusive importance gradually diminished, and scope of their work underwent changes accordingly. Still, they

remained relevant in certain specific workspaces that required their expertise.

Khalasis were used traditional methods and equipment such as wooden beams, coir ropes, chain blocks and *kappi* to lift and move heavy loads. Their specialized knowledge and skill in handling such equipment allowed them to control and manage extensive weights effectively. All works was led by their *Muppan (*Head of particular *Khalasi* group) and they performed challenging tasks with the utmost dedication. Their settlements were mainly concentrated in the coastal areas, from the southern regions of Malabar to the northern parts. They strategically chose locations that offered significant work opportunities. *Khalasis'* local knowledge and expertise in dealing with various issues helped them efficiently execute their work tasks, which varied depending on regional requirements. They adapted their work based on the specific challenges and opportunities present in each region.

The nature of jobs is that *Khalasis* used to handle heavy mechanics. They were skilled laborers using various tools and equipment to lift heavy objects and transport them from one place to another. With the help of simple tools and their experience, they were capable of carrying out demanding tasks efficiently. They were highly esteemed in their profession (Muhammad Sadham Chaliyam, 2013, 120). During the modern period, traditional occupations transformed and modern machinery took over many tasks in different industries. However, *Khalasis* remained relevant and adapted to the changing times by embracing modern technology and integrating it into their work. Despite the shift in job roles, their expertise in handling equipment and their skills were still highly valued. Over the years, *Khalasis* have established their flexibility by effectively incorporating modern machinery into their work without losing their traditional importance. They continue to be an integral part of society, living with great significance and contributing to various industries without losing their essential skills.

From the early days, Beypore served as the primary center for shipbuilding in India, and this is why the *Khalasi* community became

more centralized in this region. Their skills were essential for both ship construction and later launching the ships into the sea. They possessed the expertise to handle heavy loads on both land and water. *Khalasis* were adept at performing challenging tasks in the sea and on the coast with equal competence. There are two divisions within the *Khalasi* community. One division is involved in land-based works, including railway work, construction, huge flat air condition work, factory machine erection work, and rescue operations at sites where accidents involving vehicles occur. Their knowledge and competence in managing complicated tasks that were beyond the capabilities of machines were recognized throughout different parts of Kerala. In regions such as Chaliyam, Karuvanthiruthy, Feroke, Thazhekkad, Pakkumkara, Muzhuppilangad, Valapattanam and Kannur. *Khalasis* were involved in various works related to shipbuilding and harbors.

From Tradition to Present: How the Khalasis are Staying Relevant

Khalasis, who had been involved in the construction of ships in Beypore, has a rich history and a deep-rooted connection with the traditional knowledge and skills passed down through generations (personal Interview, Ummer Muppan, 12th December, 2022). Their traditional technical skill and dedication have earned them immense respect and admiration, not only in the local community but also globally. Their contribution is being recognized even beyond the boundaries of Malabar. However, as industrialization and European influence brought changes to Kerala's socio-economic scenario, they adapted to the evolving times. With the advent of modern machinery and the impact of colonialism, they expanded their expertise to embrace new professions and industries. During the colonial period *Khalasis* played a significant role in shaping the traditional craftsmanship of Kerala and creating new opportunities to excel in diverse fields ((Muhammad Sadham Chaliyam, 2013, 121). *Khalasis*, with their diverse skills and adaptability, have managed to maintain their relevance and significance in various industries. Both within and beyond their traditional domains, making them a respected and valued community in Kerala's social fabric.

During the time of British rule in India, *Khalasis* played a significant role in various railway construction activities. They were involved in heavy work such as building rail tracks, bridges, and large factories where heavy machinery was installed. Their expertise was beneficial for many government projects in Kerala. The British government relied on *Khalasi* services not only in Kerala but also in other regions. Gradually *Khalasis* gained recognition and were known for their exceptional skills, both within and outside Kerala. They were sought after by organizations beyond colonial India for their technical expertise in handling large-scale projects. In the colonial period, when India witnessed several major construction projects, *Khalasis* technical skills were highly valued. Their ability was manifest in the construction of massive railway bridges and huge dams, showcasing their engineering capabilities. *Khalasis* played a vital role in the infrastructure development of India during the British colonial period, with their technical skills being highly appreciated and recognized in various significant projects.

During the time of the First World War, there are references in some British records suggesting that *Khalasis* were employed for heavy work in railway construction outside India. It was mentioned in discussions related to the construction of the Bara-Basra Mesopotamia railway line that Chaliyam *Khalasis* were used for this purpose (personal interview, Hassan Koya, 26th January 2023). The British records mention that the *Khalasis*, who cooperated very effectively in the construction of the railway, were given leased land in the coastal region of Malabar as a token of appreciation. Projects like the Kadalundi Bridge and Mettur Dam are some examples of the early works undertaken by *Khalasis* during the colonial era. The construction of the clock tower in Mecca (The Clock Tower in Mecca is a prominent land mark and a symbol of the city's identity. It is officially known as 'Abraj Al Bait Clock Tower. It is visible from various parts of the city and serves as a reference point for millions of pilgrims who visit Mecca during Hajj and Umrah) is another example of the work undertaken by *Khalasis* .(personal interview, Muhammed Koya, 23rd April, 2022)

In the activities related to the sea, another essential division of the *Khalasis* was their involvement in the construction and

maintenance of wooden boats in the region of Malabar. In the early days, certain circumstances large ships were unable to navigate directly to their destination. It was during such situations that the *Khalasis* played a crucial role in navigating and steering the boats. In the early days large wooden boats were used for transporting goods, especially spices, sandalwood and other precious products. Due to their size and design, they were unable to reach the harbors directly. In such cases, the *Khalasis* were responsible for guiding the boats and maneuvering them to reach the nearest harbor. These skilled individuals had an exceptional understanding of the sea and the local waterways, allowing them to safely navigate the boats. Their expertise was also valuable when loading and unloading cargo. They ensured that heavy goods and materials were handled efficiently and securely during the process. Additionally, their proficiency in handling heavy objects was a significant asset when lifting and elevating items on both land and sea. The major areas where we can find *Khalasis* involved in such activities related to the sea are Chaliyam, Beypore, Kallayi, Ponnani, and Tirur. They possess specific regional expertise and utilize technological skills that we can observe in each of these regions (personal interview A Najeeb 30th November 2022).

The *Khalasi* of Beypore gained worldwide recognition, and one of the most significant events in their history was the Peruman train accident in 1988. Mappila *Khalasi* from Beypore, Chaliyam and Karuvatthuruthi regions had actively taken part in the Peruman rescue mission (Personal interview, Ummar Muppan 2nd November, 2022). The technology of the traditional *khalasis* was not yet well known to the general public. They showed the world in the face of disaster how heavy things could be lifted using their traditional weapons. The *Khalasis* took up the task when all the rescue operations launched with the help of heavy machinery could not be successful. The *Khalasi* of Beypore and Chaliyam were able to lift the bogies with relative ease when several modern engineering techniques failed to retrieve railway bogies from the depths of the lake (Alex George, May 6, 1989, *Economic and Political Weekly,* p.965)

From the beginning the Indian Army's Armed Recovery Vehicle took over the rescue mission. So, the *khalasis* were not directly

involved in the rescue mission. However, even then, they played a crucial role in helping the army climb up by fixing iron ropes on the bogies sunk several feet below the water surface. But the attempts to lift the train using crane failed. The mission failed when the iron rope tied to the bogie to lift it broke. Rail coaches were gone under the water again. The *Khalasis* then took over the responsibility of lifting the bogies. In this critical situation, the Mappila *Khalasi* used their traditional tools such as *kappi* and rope, for this rescue operation (Personal interview, Ummar Muppan 2nd November, 2022). However, initially, the railway engineers did not have much faith in the skills of the *khalasis*. The Khalasis, with their strenuous efforts, pulled out the railway bogies one by one from the water. The people present watched the work of the *khalasis* with great wonder.

Unique Cultural expression's

In Beypore, *Khalasis* have an exceptional role in the construction of traditional wooden boats known as *Uru*. Due to the long history of *Uru* construction, they have a rich heritage and experience in this field. They have been involved in building *Uru.* Their expertise is especially significant in the construction of traditional wooden boats, which is a unique aspect of their craft. The *Khalasis* of Beypore play a crucial role in launching the newly constructed *Uru* into the water. This task requires a specific set of skills that are mastered by the *Khalasis* through their long-standing involvement in the *Uru* making process. In addition to their involvement in sea-related activities, *Khalasis* were skilled in handling large boats that entered the harbors. When such boats got stuck in the area of little water, the *Khalasis* themselves were capable of maneuvering and freeing the vessels. To accomplish such tasks competently, *Khalasis* relied on their special tool called "*Dhawar*" commonly known as a wooden *vinch*. Along with *Dhawar*, *Khalasis* used additional tools such as "*kappi*" and "coir" to aid in their effort (C.P Musthafa, 2019 p.338). Their expertise in using these tools made their work much simpler and more efficient. Several traditional songs and chants associated with their heavy work are known as "*Vinchi pattukal*" "*Amba pattukal*" and "*Elayya pattukal*," which signify their historical

connection with their profession (personal interview with Muhammed Koya, 23rd April, 2021)

Due to the serious nature of their work, a sense of solidarity among the laborers becomes crucial. Providing inspiration and enthusiasm to the workers is the purpose of such songs. Often, these songs aim to simplify challenging tasks and elevate the mood of the workers. The rhythm and melody of these songs were designed to invigorate the laborers, encouraging them to work with more energy and dedication. (B. Muhammed Ahammed, 2006, 52). These songs create a sense of unity and shared experience among all the workers, making them feel more connected and driven to achieve their common goal. When we study the history of work songs, we can indeed observe a uniform nature. All types of songs used in workplaces aim to reduce the burden of labor and foster amity among the workers. The use of work songs created a sense of collaboration and cooperation among the workers, leading to a collective effort in achieve their goals. The lyrics of these songs were not purely for artistic purposes; rather, their significance lay in motivating the workers and creating a sense of solidarity within the workforce. So, the lines of these work songs did not follow the conventions of refined music; instead, they prioritized the essential message of unity and encouragement. Workplaces are filled with various emotions, joys, sorrows, and challenges. All of these characteristics are reflected in the work songs, making them an integral part of the work environment.

The work songs sung by the *Khalasis*, who were involved in the construction of Beypore *Uru* are known as "*Panipattu*" or "*Kappal* p*attu*." These songs hold significant impact of the *Khalasi* Muslim community, which was engaged in the different stages of *Uru* building activities (personal Interview, Ummer Muppan, 12th December, 2022). The style of singing and the vocal techniques used in these songs were influence by *Mappila pattu*. The lyrics song contains references to *Allah*, the divine power, reflecting the deep faith and spirituality of the workers. The *Panipattu* or *Kappal pattu* was not limited to just artistic expressions. They served a greater purpose in creating a sense of unity and strength among the laborers. These songs incorporated the legends of Prophet Muhammad,

*Karamat (*Arabic term commonly used in Islamic religious context to refer the miracles or extraordinary acts performed by saints or holy person. These miracles are believed to be manifestations of divine power and are often considered as signs of the person's spiritual and connection with God) of Sheikh or *Auliyas*. *Panipattu* or *Kappal pattu* played a significant role in the work environment. It bringing together the workers and motivating them to carry out their tasks with determination and unity.

The chief purpose of the *Khalasis* using work songs is to gain energy and motivation for their work. These songs provide a source of strength for the workers. The term commonly used to refer to those who sing work songs is known as "*Ambakkaran*". The leader of the group is called "*Khalasi Moopan* who acts as *Ambakkaran*". '*Jawabmar'* as the term used to refer to those who respond to the song or repeat it is sung by *Ambakaran*. Their usage of specific words and context depends on the situation and the demands of the work environment (personal interview with Mammu,15th December, 2022). Some of the work songs may contain short poetic verses, and they are used accordingly based on the rhythm or tempo of the work. Various workers may sing the same song, but the lyrics may be adapted to fit the context of the different work sites.

This paper mainly focuses on the distinct style of *Amba* songs. When analyzing the lyrics of these work songs and examining the techniques used, it becomes possible to gain a clear understanding of the different work environments. *Mappila Khalasi Katha parayunnu* the malayalam work written by C.M Mustafa Haji Chelembra discusses the detailed references to the unforgettable experiences of the *Khalasis.* In this work, Chelembra narrates the details of the strenuous work that *Khalasis* undertook using traditional equipment called *Vinchi* to lift weights at the construction sites in Malabar (C.M Musthafa Haji Chelembra, 2011, pp.37-40) Before attempting to lift a heavy object, the experienced *Khalasi* in the group would call out "*Pidikkalle*" (going to lift) to which others would respond. Then the lifting process started and everyone joined together (C.M Musthafa Haji Chelembra, 2011, pp.37-40). After that throughout the work, they would continue singing the *Amba Pattukal.* Everyone, hold it and lift

it together. The *Khalasis* would engage in the laborious task while singing *Amba Pattukal*, making their work more manageable and inspiring each other with a sense of unity. Some lines from the *Amba paattukal* that the *Khalasis* used to commonly use in their workplaces are mentioned in this context.

Ailasa… ailasa….

Oblamali ailsa…

Thalla pokkaru ailasa…

Ailasa… ailasa… (personal interview, Abubaker , 18th December, 2022)

It is impossible to find the exact literary meaning of lines mentioned above. The workers sing these lines together, called "*ailasa*," to make the task of lifting heavy objects more strenuous. It is more likely that the term "*thalla pokkar*" refers to an imaginary leader. Such *amba* songs were used during times of heavy lifting and also during times of pulling or pushing heavy loads.

We can see different kinds of amba *pattukal* that the *Khalasis* used to sing, depending on the nature of the work. The nature of the song totally different when they sang it during rescue operations at accident sites. Here is the translation of the famous lines from the *amba pattukal* sung by Khalasis during vehicle accidents and rescue operations:

Vandi marinje …ailasa..

Undikkettu ailasa…

Ailasa…ailasa

Oblamali ailasa.. (personal interview, A Najeeb, 30th November, 2022)

The words "*vand*i *marinje*" and "*unthikettu*" are in the traditional common usages."*vandi marinje*" means that the vehicle has overturned. "*unthikettu*" refers to the collective effort of lifting a fallen vehicle using everyone's strength. Khalasis commonly use *ailasa* calls in all kinds of heavy lifting tasks to reduce the workload.

Kallayi River (Kallayi puzha is merge with the Arabian Sea in Kozhikode. The river is significant for its historical and cultural importance) which was strongly connected with the lives of *Khalasis*

in Malabar. In the trade history of Malabar Kallayi River was considered the main center of the ancient timber trade. The main theme of the *amba pattukal* revolves around the Kallayi river, as it had a profound impact on the professional and social lives of the Khalasis. From the song of a*mba Pattu*, we can assume how much influence and impact the Kallayi River had on the lives of *Khalasis*.

Allante kamalu rahmathu
Thannalu rabee barakkathu
Allante kamalu rahmathu
Thannalu rabee barakkathu
Kallayippuzhayude rahmathu
Thannalu rabee barakkath (*personal* interview, Hussain P , 26th January, 2023)

The Kallayi River was an integral part of the lives of *Khalasis* in Malabar, and it played a significant role in shaping their livelihoods. It served as a major center for their activities, and they depended closely on the river for various stages of their lives. The main thing that is being indicated in these lines is that the biggest blessing that God has given to the *Khalasis* is the Kallayi River. This song "*amba pattukal*" reflects the association between *Khalaasis* and the Kallayi River, symbolizing the wealth and prosperity bestowed upon them by God.

Another important place where the Khalasis sang amba pattukal was in connection with the different stages of uru making. Khalasis used to be involved in all the stages of Uru making. The Khalasis themselves used to do all the different heavy-duty tasks related to Uru construction. In all these stages, the *Khalasis* used to sing *vinchi* songs to lighten their workload. During the time of *Uru* launching in to the sea, the *Khalasis* sang a song to ease their fatigue from laborious work (personal interview, Ummer Muppan, 12th December, 2022). During this period, they sang song known as *vinchi pattu*. In these vinch songs, everything that brings enjoyment and comfort to the mind will find its place in the lyrics. They used *vinchi pattu* song inspired by Muhiyudheen Sheik's extraordinary skill. They believe that Muhiyudheen Sheik's exceptional abilities would bring about more

significant accomplishments in this meticulous endeavor (personal interview, Ummer Muppan, 12th December, 2022).

Alla alla ya salama
Porishayerum nurudheen sheik
Ya auliya
Alla allay a salama (personal interview, Mammu, 15th December, 2022).

It is possible to witness profound songs in the *vinchi* tradition, expressing deep religious sentiments in the cultural history of Malabar. *Auliyakkal* played a significant role in shaping the strong beliefs and cultural values in Malabar. Hence, we can indeed have an enormous collection of poignant *vinchi* songs.

Shahid abubakkar samadani oliyulla
Allahi alla salamu
Shahid abubakkar samadani oliyulla
Allante alla kaval
Shahid abubakkar samadani oliyulla (personal interview, Hussain P ,26th January, 2023).

We can see many *vinchi* songs that mention the miracles of the *Auliyas*. In such songs, we can see the *Auliyas* being praised in an immense way. The *Khalasis* believed that when doing heavy work, the *Auliyas* would be with them and help them lift the weight invisibly. This belief gave them the confidence to lift even the heaviest objects.

The existence of such *Amba paattukal*, which praised *Allah* (God) and the *Auliyas*, was another important proof of the strong faith that the Mappilas possessed.

Alla alla…yallaa…
Keripokatte ya allaa
Alla allay a alla…

The song *Ellayya pattukal* was commonly used by *Khalasis* to lift heavier loads during manual labour. In some places, these types of work songs were also known as *amba pattukal* or a*layya pattukal*. These songs provide rhythm and motivation for the workers, making

it easier for them to coordinate their efforts and lift heavy weights together.

Othupidichal malayum porum elayya
Kakkane njangale ellayya
Pavangalan elayya
Mureed auliya ealayya
Alla alla elayya
Kakkane alla elayya
Muthu nabiye elayya

Each *Elayapatt* or *Ambapatt* song provides valuable information about the lives of Khalasis. By analyzing the *Elayapatt* songs mentioned above, we can find facts that support these observations. *Othupidichal Malayum Porum:* The phrase "*Othupidichal malayum porum"* means that if we stand together, even an impossible task like breaking a mountain becomes easy. This reminds us of the importance of unity and cooperation among the Khalasis. They were a community that worked hard together and helped each other.

"*Kakkane njangale ellayya- Pavangalan elayya -Mureed auliya elayya*" we see the poor *Khalasis* praying to the saints (*auliya*) for their protection. *Khalasis* himself says that they were very poor and they faced many hardships. Therefore, they believe that the help of God and the saints is essential for them. It is clear that, through such *amba pattukal*, they greatly desire the mercy and compassion of God. Songs like ambapatt and elayapatt reveal important details about the social, cultural, and economic standing of *Khalasis*. These songs give us a clear picture of their unity, cooperation, faith in God, poverty and hardships. They serve as an important source for understanding *Khalasi* culture.

Allase ele mali
Allase ele chumbra
Allase ya maoulani
Allase musakka
Allase beeran ponni
Allase maveli nattil

Allase vilayatt undedo (personal interview, Ubaith , 15th December, 2022)

The *Khalasis* used to sing a large number of work songs that were widely common at the work sites. These *amba pattukal* (work songs) played a vital role in the lives of *Khalasis*, providing them with much-needed relief during their laborious tasks. With the help of these songs, they could synchronize their efforts while lifting heavy weights and the rhythm of the songs made their work more manageable and inspiring. The songs were used in conjunction with their work routines. The *Khalasis* adjusted the lyrics of the songs based on the nature of their work and the difficulty of the task. Depending on the specific work, they used different verses and adjusted the tune accordingly. For example, they sang *Bhakti Pattukal* (devotional songs), *Hasya Pattukal* (comical songs), and *Theri Pattukal* as per the context of their work (personal interview, Ubaith , 15th December, 2022). Many types of songs were frequently sung in accompaniment to *Amba paattukal*. The enchanted verses of these songs embodied humor, faith, and life itself. *Khalasis* unity is the most significant component of their work. When a *Khalasi* in a group is not giving his work his full attention, the other members of the group tease him and sing about it. Such lines were quickly making their way into their songs. In the same way, occasionally they would pair these songs with swearing songs. Such swearing songs were regarded by them as a type of workplace humor. All those involved in the *Khalasi* profession were part of these songs. The truth is that these songs, whether they were swearing songs or mocking songs, never had an adverse impact on the *Khalasis* sense of unity.

Conclusion

The unique and outstanding feature of *Khalasi* culture is the representation of their work songs, known as "*amba pattukal*." These songs have a deep-rooted connection with the cultural life of the *Khalasi* community in Kerala. Regardless of the nature of the work, the *Khalasis* used these songs to efficiently coordinate and manage their labor-intensive activities. These songs were a perfect example of how work and cultural practices could intertwine harmoniously.

Even the *Vinchi Pattukal* served as a cultural representation of traditional community practices. The *Khalasis'* social group in Malabar exhibits a strong cultural unity, heavily influenced by their beliefs, customs, and rituals, which are reflected in their lives. These songs also brought out their talents and showcased their traditions through competitive representation. Irrespective of regional differences and variations in work types, the *Khalasis* demonstrated unity by coming together to sing and perform during laborious tasks, making these work songs a significant aspect of their cultural heritage. Throughout different regions and diverse work assignments, the *Khalasis* maintained their unique cultural identity by integrating these labor songs into their work routines. This tradition of using work songs has been passed down through generations, allowing them to preserve their customs and beliefs. The notable ability of the *Khalasis* to adapt their work songs to different contexts and work environments highlights their creativity and resilience. Whether it was a representation of *vanchi pattukal* or *Amba pattukal* to demonstrate their cultural heritage and bring together diverse beliefs and practices. These work songs, such as *Amba pattukal*, play a vital role in the *Khalasi* community, representing their culture, customs, and collective spirit. The songs serve as a reminder of their shared heritage and inspire unity among *Khalasis* making them an essential element of their cultural identity.

Bibliography

Personal Interviews

Abubaker Valyattil (63), Khalasi worker, Beypore, 18th December, 2022
A Najeeb (68) , Khalasi worker, Feroke, 30th November 2022
Hassan Koya, Khalasi Muppan, Chalyam, 26th January, 2023
Hussain P (76), Khalasi Muppan, Chaliyam, 26th January, 2023
Mammu (72), Kahalasi worker, Karuvanthuruthi, 15th December, 2022
Muhammed Koya, (65) Khalasi Muppan, Beypore, on 23rd April, 2022
Ummer Muppan,(67) Kalasi Muppan, Beypore, 12th December, 2022
Ubaith (62) , Khalasi worker, Karuvanthurthi, 15th December,2022

Works Cited

Alex George, (May 6, 1989) Malabar *Khalasis' Traditional Technology to the Rescue in Perumon*, Economic and Political Weekly, Vol. 24, No. 18, 1989, pp. 965-967

Muhammed Ahammed, B. (2006) *Mappila Folklore*, Samayam publication ,Kannur

Musthafa, C.P. (2019) *Khalasi Kayika Vaidagdathinte Mappila Paithrikam*, Proceedings of Kannur Muslim Heritage Conference, Kannur

Musthafa Haji Chelembra, C.M, (2011) *Mappila Khalasi Kadha Parayunnu,* Pradheekksha books, Kozhikode

Sadham, Muhammad, Chaliyam, (2013) *Chaliyathinte Charithra Chalanangal*, Majlis offset printers, Calicut

Ms. Nasreena P.K
Assistant Professor of History
S E S College, Sreekandapuram, Kannur
India
Pin: 670631
Ph: +91 9744809808
Email. nasreenapk0@gmail.com
ORCID: 0009-0008-0792-5192

MRS Advances
https://doi.org/10.1557/s43580-024-00888-z

ORIGINAL PAPER

Effect of precursors in the supercapacitor performance of g-C_3N_4

Vattakkoval Nisha[1,2] · Fabeena Jahan Jaleel[1] · Manjacheri Kuppadakkath Ranjusha[1,2] · Padinjare Veetil Salija[1] · M. Neethu Raveendran[3] · Anjali Paravannoor[1] · Baiju Kizhakkekilikoodayil Vijayan[1]

Received: 15 April 2024 / Accepted: 20 May 2024

Abstract

The present study demonstrates the synthesis of sulfur-doped 2D graphitic carbon nitride (T-CN) from thiourea as a precursor and its enhanced electrochemical properties as a supercapacitor electrode. An elaborate study has been carried out to elucidate how the structural and morphological characteristics of the material affect the electrochemical performances of the samples and subsequently their performance as a supercapacitor electrode. The results were also compared with pristine graphitic carbon nitride samples sourced from urea (U-CN). For the T-CN samples, a specific capacitance value of 566 F/g was obtained at 3 mV/s, which is an increment of more than fivefold as compared to U-CN (115 F/g). The energy density value of the T-CN sample was as high as 41 Wh/kg at a power density of 2.2 kW/kg.

Introduction

Supercapacitors have drawn the attention of a broad and expanding variety of fields, which include electronics, industrial power, energy management, and mobile electrical systems [1]. Supercapacitors as energy storage devices have recently gained popularity due to their promising properties such as higher power density, prolonged life time, quick recharge potential, environmentally sustainable characteristics, and so on [2]. They are now highly valued in the worldwide energy sector due to their high energy density, outstanding stability, and exceptional efficiency. Although batteries have a high energy density, they take longer to charge than supercapacitors. Generally, supercapacitors have reduced the gap between batteries and conventional capacitors. Supercapacitors are capable of storing and releasing energy at an extremely fast rate, as well as delivering a large current in a short period of time [3, 4].

Supercapacitors are classified into three types. The first one is an electrical double-layer capacitor (EDLC) which achieves capacitance by accumulating pure electrostatic charge on the electrode–electrolyte interface. The second type of supercapacitor is the pseudocapacitor, which undergoes a fast and reversible faradic process due to electroactive species. The third type is a hybrid, which is the combination of both EDLC and Pseudocapacitors.

Major troubles faced by supercapacitors are the low energy density, high cost of production, small voltage per cell, and high self-discharge. The electrode material chosen is another critical factor as it defines the electrical properties of the device [5]. Hence, researchers are seeking ways to boost the capacity as well as the overall performance of supercapacitors by utilizing various electrode materials including carbon, transition metal oxides, conducting polymers, sulfides, Mxene, or a combination of these materials based on their intended uses [5, 6].

Due to their outstanding optoelectronic and electrocatalytic properties, two-dimensional (2D) materials have expanded the frontiers of materials science, making research into solar energy conversion and storage devices, more common compared to ever before [7]. In recent decades, carbon nitride have received a lot of attention as a new two-dimensional material. There are five allotropic forms of carbon nitride: α-C_3N_4, β-C_3N_4, graphitic-C_3N_4 (g-C_3N_4), pseudo-cubic, and cubic C_3N_4 [3]. g-C_3N_4 is a commonly used allotropic form owing to its stability. Its aromatic structure with lone pairs of electrons can

✉ Baiju Kizhakkekilikoodayil Vijayan
baijuvijayan@kannuruniv.ac.in; baijuvijayan@gmail.com

1 Department of Chemistry/Nanoscience, Kannur University, Swami Ananda Theertha Campus, Payyannur, Edat P.O., Kannur, Kerala 670327, India

2 Department of Chemistry, Payyanur College, Payyanur, Kannur, Kerala 670327, India

3 Department of Chemistry, Sir Syed College, P.O. Karmbam, Taliparamba, Kannur, Kerala 670142, India

Published online: 03 June 2024

increase the polarity and mobility of charge carriers in electrochemical systems for energy storage [8]. 2D g-C_3N_4 nanosheets are widely studied in supercapacitors due to their high specific surface area, porous structure, and short ion and electron transport paths [9]. In contrast, the chemical inertness and low conductivity of pure g-C_3N_4 limit its applications in many fields.

As a result, most researchers have concentrated on alterations of g-C_3N_4. The methods of alteration in the structure of g-C_3N_4 are classified as in situ synthesis and post-treatment. The three major post-treatment methods are liquid exfoliation, chemical oxidation, and protonation. Yet, these methods yield only small amount of g-C_3N_4. To synthesis g-C_3N_4 and its composites with enhanced chemical activity and large specific area, in situ modification routes such as copolymerization and element doping have been developed [10]. The chemical and electrical characteristics of carbon hosts can be improved by doping with heteroatoms like phosphorus, boron, sulfur, and nitrogen, resulting in increased energy storage ability [11]. The doping of heteroatoms (for example, B, N, P, S, and others) into the matrix of carbon can generate certain additional contributions from pseudocapacitance to increase total capacitance and even improve the ion diffusion at the electrode/electrolyte interface. For instance, MacFarlane et al. synthesized N-doped mesoporous carbons with a large surface area by direct co-pyrolysis of calcium citrate, sodium citrate, and benzimidazoliumtriflate salts at 850 °C. Kang et al. also synthesized N-doped porous carbon by pyrolyzing magnesium citrate and then treating it with NH_3, and it was used as a cathode in a high-power lithium ion supercapacitor [12, 13]. Feng et al. summarized that carbon materials doped with heteroatoms are used as the most promising candidates for a variety of applications, including oxygen reduction reactions, supercapacitors, and batteries [14].

In recent years, sulfur-doped carbons have grown as the electrode materials for supercapacitors. Sulfur-doped carbons perform better because of the electron-rich aromatic sulfide, which offers a highly polarized surface under the influence of an applied electric field, leading to a higher electrolyte dielectric constant and making the charge transfer process. Furthermore, the presence of sulfone and sulfoxide species causes a series of redox faradic reactions on the sulfur-doped carbons, resulting in increased pseudocapacitance [1]. Furthermore, sulfur contributes significantly to the specific capacitance and stability of a supercapacitor with several sulfur vacancies and impurities. So sulfur doping in g-C_3N_4 is a very appealing approach to creating an efficient supercapacitor electrode material [15]. A systematic comparison and analysis between S-doped C_3N_4 and C_3N_4 was conducted in the manuscript.

Experimental

Reagents and materials

Urea (Merck, 99%), thiourea (Alfa Aesar, 99%), ethanol (Sigma Aldrich, 96%), Isopropyl alcohol (SRL, 99.5%), Nickel nitrate (Merck, 98.5%), Potassium hydroxide (Merck, 85%), and Nickel foam were used directly without purification.

Synthesis of U-CN and T-CN

The two samples U-CN and T-CN were synthesized through thermal polycondensation of urea and thiourea, respectively. In a typical procedure, 10 g of urea was weighed in a silica crucible. 20 ml of ethanol was added to this to dissolve it. After that, the crucible is closed with a lid and placed into a hot air oven at 80 °C for 24 h. The product formed was put into a muffle furnace, setting the temperature for 550 °C at the rate of 2.3 °C per minute. The synthesized U-CN sample was washed with 0.1 M HNO_3 and distilled water. Then, the sample was dried at 80 °C [16]. The above-mentioned procedure was followed for the synthesis of the T-CN sample in the place of urea, thiourea was used.

Fabrication of electrodes

The two electrodes were fabricated through electrophoretic deposition (EPD) 0.20 ml isopropyl alcohol was taken in a beaker, to this 10 mg of respective sample and 0.6 mg of nickel nitrate were added. This mixture was sonicated for 5 min to get a homogenous dispersion. Nickel foam (2 cm × 2 cm × 0.2 mm) substrates were put in this dispersion as the positive and negative electrodes. Nickel foam was cleaned with acetone and dilute hydrochloric acid (HCl) before use, washed with deionized water, and dried in a vacuum oven. To get a uniform coating, EPD was performed at 50 V for 10 min. Ni-foam was coated and then put inside a vacuum oven at 45 °C for 24 h.

Characterization techniques

To determine the crystalline nature of the samples, X-ray diffraction study was carried out. The crystal structure of the prepared samples was examined using a Bruker X-ray diffractometer model D8 Advance with Cu K-alpha radiation (= 1.54178 Angstrom) at a scanning rate of 0.02°s^{-1} in the 2θ range from 20 to 80°. Morphological studies of the synthesized nanostructures were performed using a Hitachi SU8010 SEM at various magnifications. The XPS study was

done by X-ray photoelectron spectroscopy using a Thermo Fisher Scientific (East Grinstead, UK) K-Alpha + spectrometer with a monochromated Al Kα X-ray source (hυ = 1486.6 eV).

Cyclic voltammetry (CV, Autolabmetrohm), Galvanostatic Charge–Discharge cycling (GCD, Autolabmetrohm), and electrochemical impedance spectroscopy (EIS, Autolabmetrohm) measurements were used to investigate the electrochemical properties of the nanosheets. The electrochemical properties of the nanosheets were investigated using a three-electrode system comprising of active material coated on Nickel foam as the working electrode, saturated Ag/AgCl as the reference electrode, Platinum as the counter electrode, and 3 M KOH as the aqueous alkaline electrolyte.

Results and discussions

Structure, morphology, composition

Figure 1a shows the XRD patterns of two samples U-CN and T-CN synthesized from urea and thiourea. Two distinct peaks were seen in XRD, indicating the crystalline nature of the two samples. The intense peak centered at 2θ ≈ 27° was associated with (002) plane, suggesting the typical interplanar stacking framework of graphitic substances. The less intense peak at 2θ ≈ 13° was attributed to (100) plane corresponding to in-plane aromatic structural packing [17–20]. In addition, the splitting of the peak at

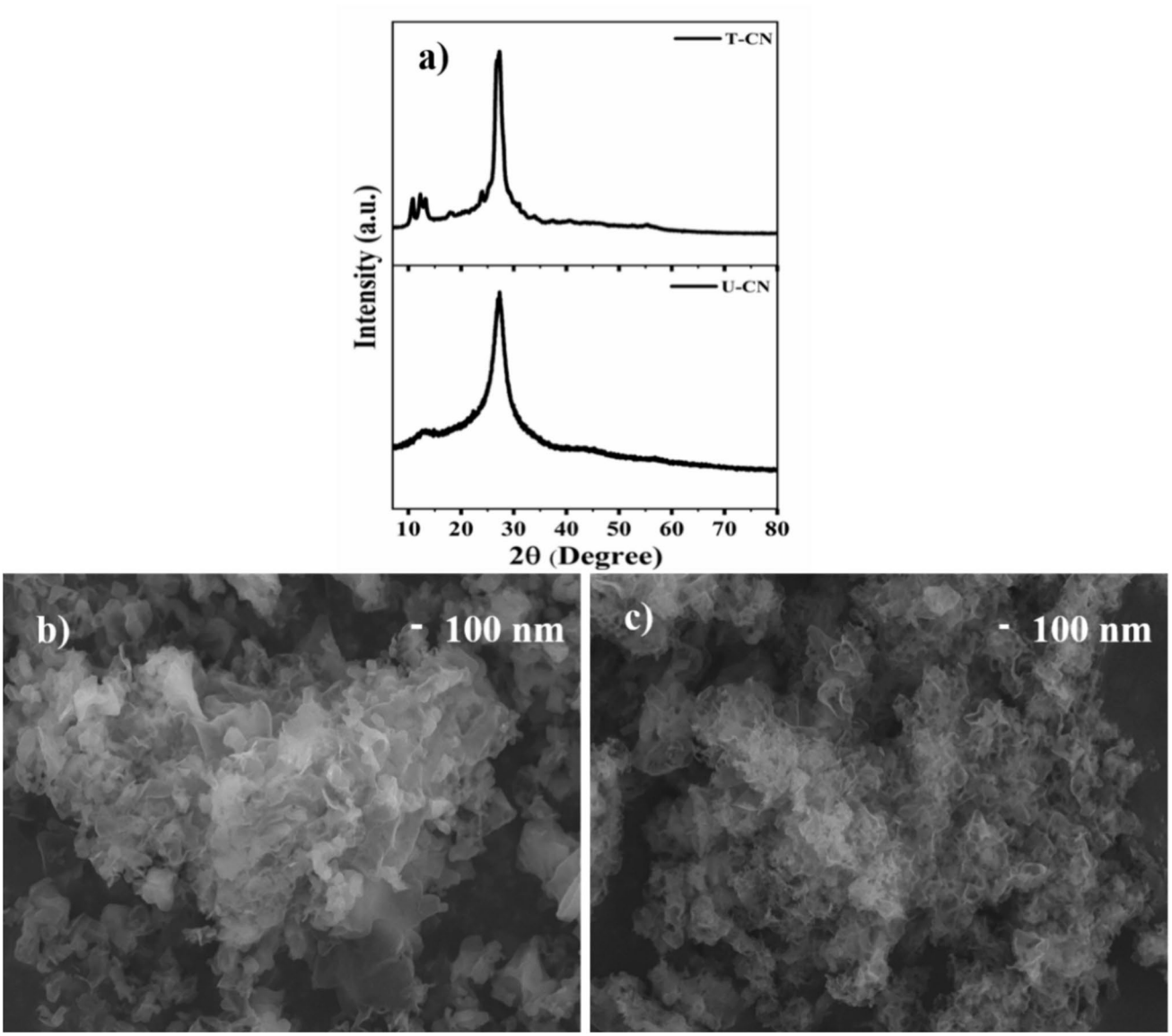

Fig. 1 **a** XRD pattern and **b** and **c** SEM images of U-CN and T-CN sample

13° in S-g-C_3N_4 has indicated the alteration of its in-plane structure caused by sulfur doping [21].

Furthermore, the diffraction peak of the U-CN sample is weaker and wider than those of T-CN, indicating the existence of a lesser crystalline nature. Urea lacks an ideal s-triazine structure and several intermediate products (such as biuret, cyanuric acid, ammeline, and ammelide) are generated in the pyrolysis process, it is difficult to form identical and well-heptazine-based g-C_3N_4, and the final product may certainly have structure defects [17, 22]. SEM images confirmed the two-dimensional nanosheet-like morphology of two samples. Ultrathin sheets of porous morphology can be seen in the T-CN sample compared with the U-CN sample. Porous morphology results in larger surface area and thereby higher capacitance [23].

The XPS spectra of the as-prepared samples are shown in Fig. 2b–e. Figure 2a represents the survey spectra of U-CN and T-CN. The four elements C, O, N, and S in samples are easily identifiable in the survey spectrum. In the C1s region, two peaks were obtained at 285 eV and 288.3 eV. The less intense peak at 285 eV was attributed to a sp^2 C–C bond caused by carbon contaminants. The presence of sp^2-bonded carbon in a nitrogen-containing aromatic ring (N=C–N) associated with the carbon skeleton of g-C_3N_4 was demonstrated by the strong peak at 288.3. The 399 eV peak is associated with sp^2 nitrogen (C–N=C) in tri-s-triazine rings. The peak at 401 eV is correlated to the amino group at the end (C–NH_2). The charging effects or positive charge localization in heterocycles are represented by the peak at 404.49 eV [24]. The peak at 164 eV in S2p spectrum is

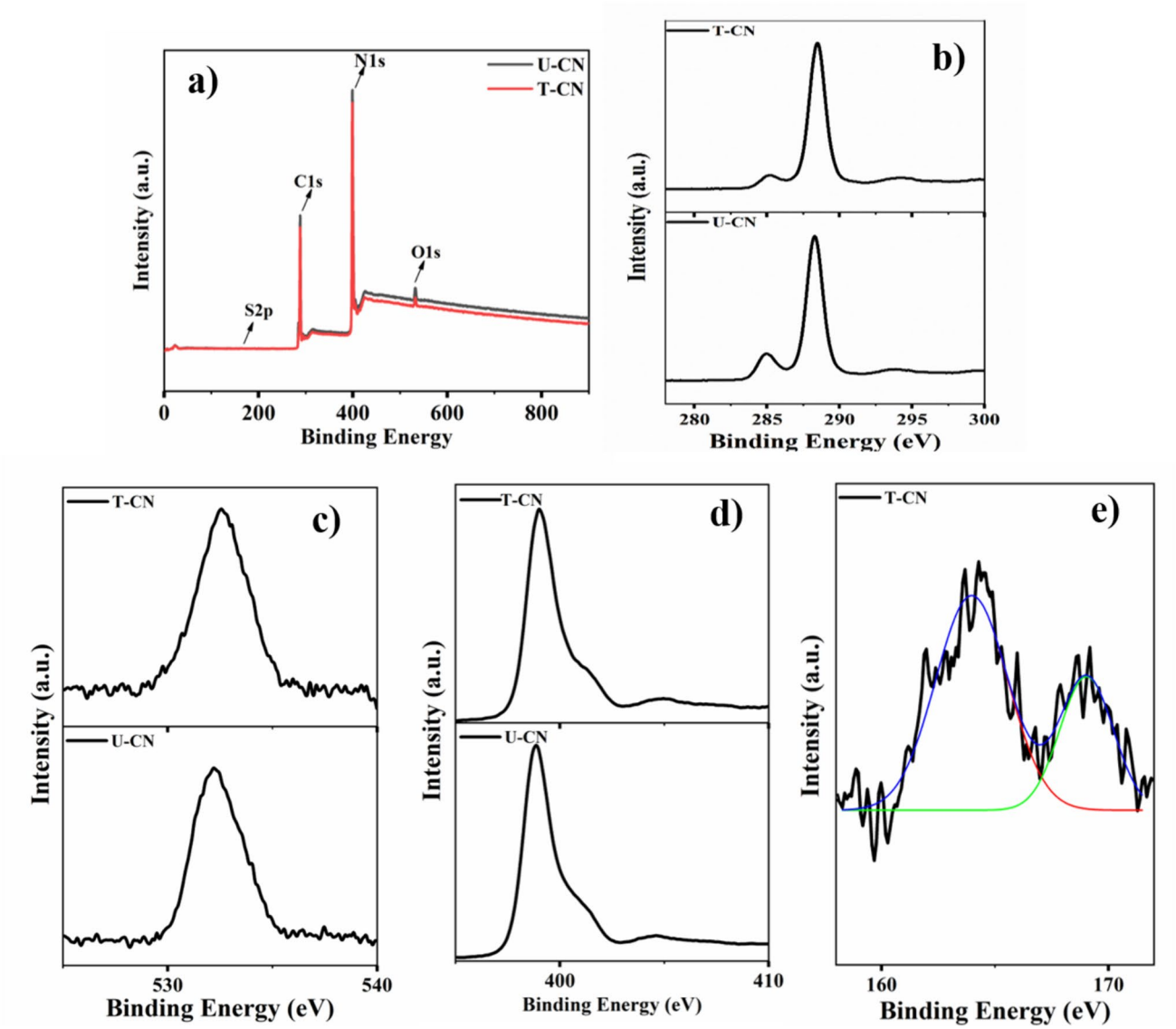

Fig. 2 **a** Survey spectrum, XPS spectrum of **b** C1s, **c** O1s, **d** N1s, **e** S2p

related to the formation of C–S bonds by the replacement of lattice nitrogen with sulfur [25] and the peak at 169 eV is ascribed to oxidized sulfur as like sulfone species resulting from the combination of sulfur and oxygen in the structure [1]. The peak centered at 533 eV is indicated to be C–N–O generated in the middle of the calcination in the presence of air [26]. The atomic percentage of sulfur is 0.2 in the T-CN sample. At the same time, the atomic percentage of N is reduced from 57.2 in U-CN to 56.4 in T-CN. These data ensured the doping of S by replacing N.

Electrochemical properties of U-CN and T-CN electrode

The samples were used to fabricate the electrodes for supercapacitor applications. The electrochemical performance of the electrodes was investigated using CV analysis in a 3 M KOH electrolyte, with a standard calomel electrode (SCE) and platinum serving as the reference and counter electrodes, respectively. The CVs of U-CN and T-CN samples are shown in Fig. 3a and b at different scan rates of 50, 25,10, 5, and 3 mV/s within a potential window of 0–0.55 V. Due to the typical pseudo-capacitive behavior of the U-CN and T-CN electrodes, broad redox peaks are displayed. A higher current density was observed with the T-CN electrode as compared to the U-CN electrode. For both samples, the specific capacitance has been calculated by using the following Eq. (1), C_{sp}

$$Csp = \frac{\int Idv}{2mv\Delta V}, \tag{1}$$

where $\int Idv$ is the integrated area under the CV curve, m is the mass of electrode material, v is the scan rate, and ΔV is the potential difference. The specific capacitance values of U-CN and T-CN are 115 and 566 F/g, respectively, at a

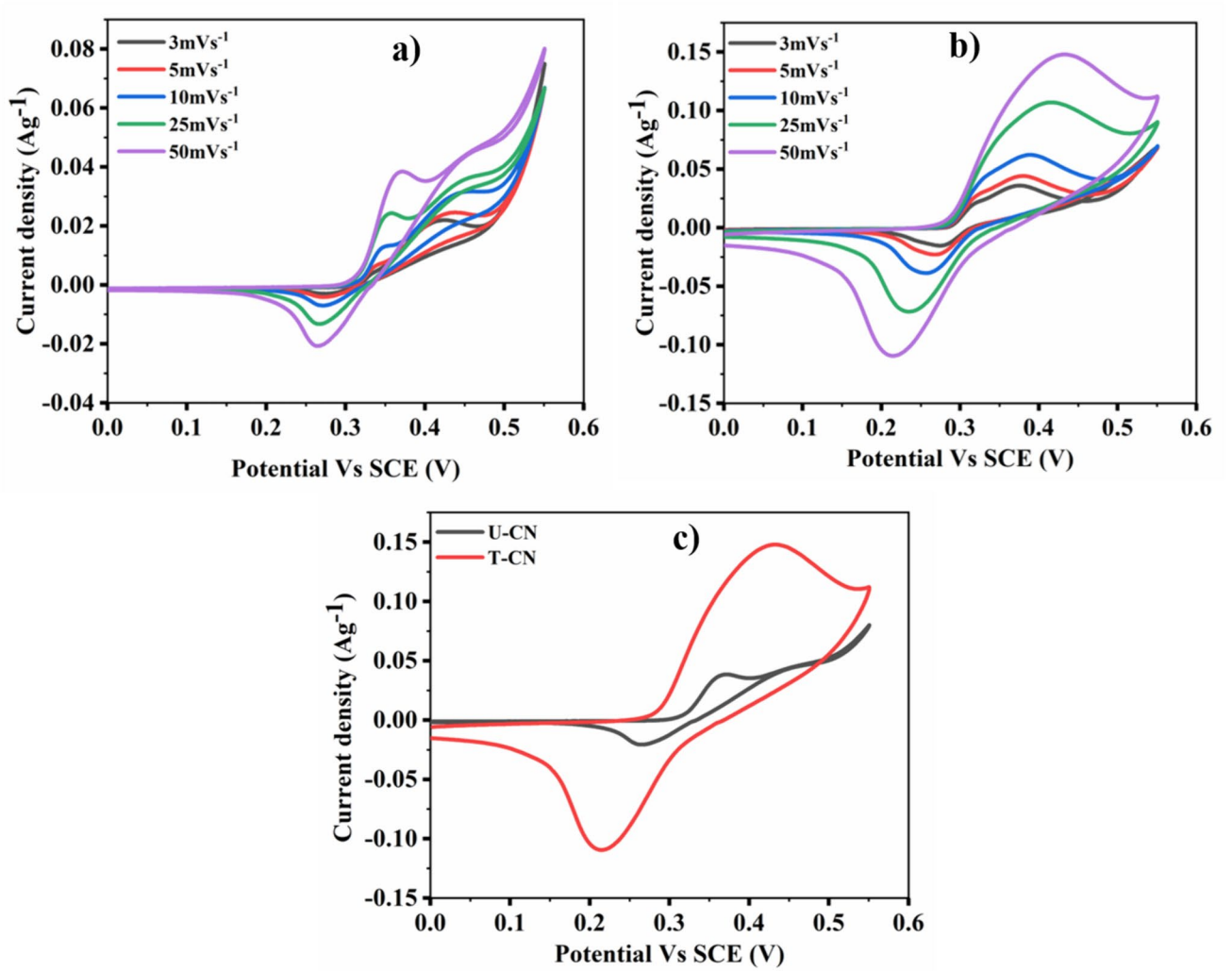

Fig. 3 CV curves of **a** U-CN, **b** T-CN, **c** CV curve of samples at a scan rate of 50 mV/s

scan rate of 3 mV/s. The perfect sulfur doping happened in the T-CN sample, with no alteration in intrinsic character, evidenced by XPS spectra. From CV analysis, it can be concluded that sulfur doping increased its electrical conductivity. Self-doping of sulfur into graphitic carbon frame work caused to have a greatly polarized surface with perfectly dispersed pseudo sites. This is the reason for good electrode–electrolyte contact and enhanced conductivity. Sulfur doping could alter the electron density and electroneutrality for high electrochemical action. The enhanced supercapacitor performance is also related to the defect formation in the carbon skeleton after sulfur doping. These defects can generate more catalytically active sites ascribed to the synergistic effects between sulfur-doped carbon nitride and the electrolyte ions [14]. Moreover, Sulfur doping was producing the C-SO_2-C group in the carbon nitride skeleton, generating the sulfone structure. The additional sulfone species could be involved in faradaic reactions and increase the capacitance of g-C_3N_4 in aqueous electrolytes. The sulfoxide group makes the compound more hydrophilic and results in pseudocapacitance [14]. And also the T-CN has activated by KOH, shows high capacitance, low charge transfer resistance and rapid ion diffusion, which was connected to its porous morphology [13].

Figure 4a and b represents the galvanostatic charge–discharge curves of U-CN and T-CN samples at different current densities 4, 5, 8, 10, and 20 mA/g. The GCD curves of the C_3N_4 electrode show an obvious deviation from the straight line, implying that the capacitance has a major contribution from Faradaic reactions rather than electrostatic interaction at the electrode–electrolyte interface. The following Eq. (2) can be used to calculate the specific capacitance of an electrode,

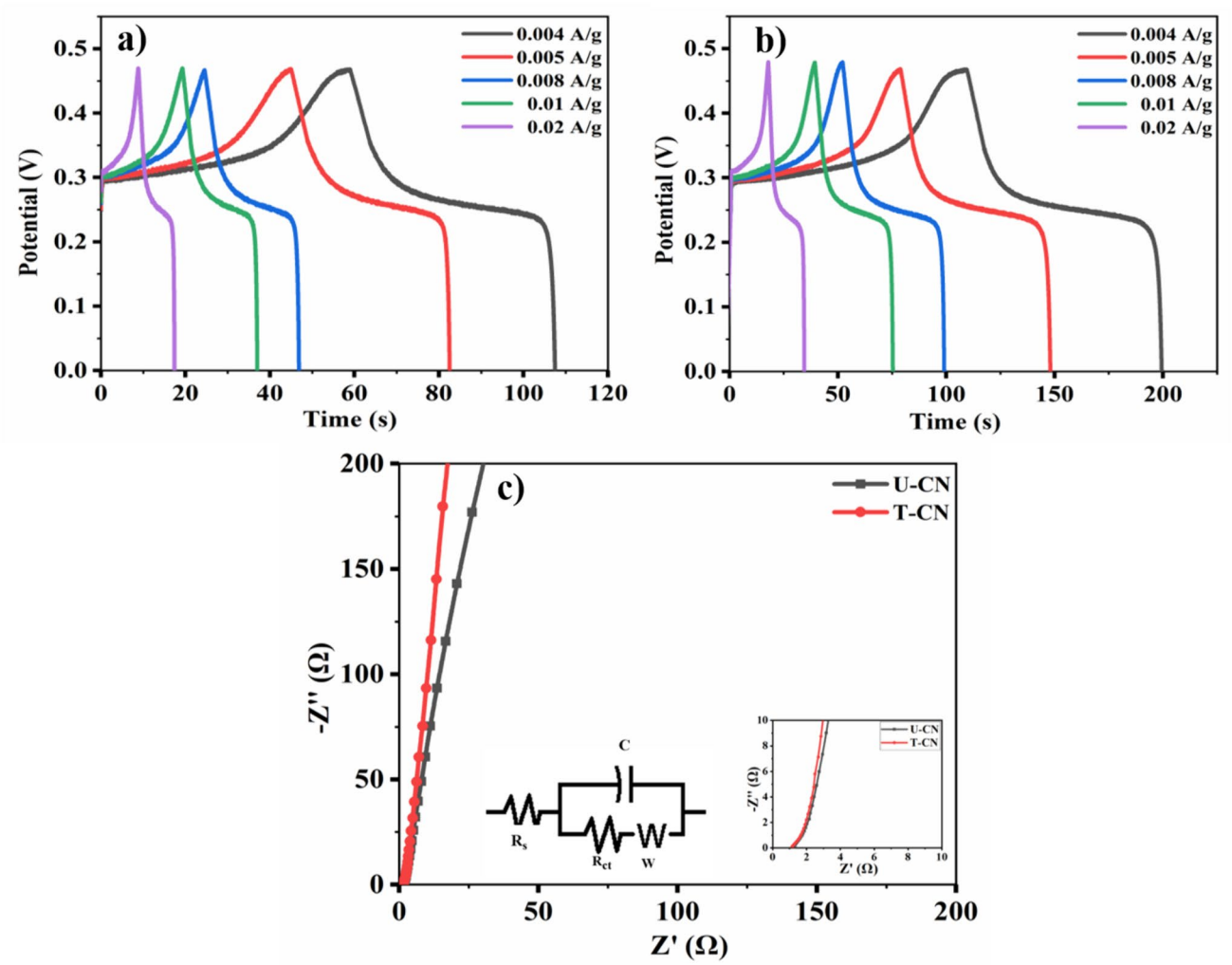

Fig. 4 GCD curves of **a** U-CN, **b** T-CN, **c** Electrochemical impedance spectra of U-CN and T-CN, inset shows the enlarge region in the high frequency and equivalent circuit

$$Cs = \frac{I\Delta t}{m\Delta V} \quad (2)$$

where I = discharge current, Δt = discharge time, m = mass of electrode material, ΔV=potential window.

The specific capacitances calculated from GCD analysis for U-CN and T-CN electrode at 4 mA/g are 115 F/g and 368 F/g.

Energy density (E) and power density (P) can be calculated by the Eqs. (3) and (4),

$$E = \frac{CV^2}{2} \quad (3)$$

$$P = \frac{V^2}{R} \quad (4)$$

The energy densities calculated for U-CN and T-CN are 13 and 41 Wh/kg, respectively, at a power density of 2.1 kW/kg and 2.2 kW/kg, respectively.

The rapid electron and ion movement of the T-CN-based supercapacitor is additionally affirmed by the Nyquist plot (Fig. 4c). The equivalent circuit for the sample is also shown in this figure. In Nyquist plot, a semicircle in the higher frequency part and a linear portion in the lower frequency part are shown. The faster ion movement between the electrode–electrolyte interface indicates better capacitive behavior of the electrodes and is evidenced by the linear part in the low-frequency region, which is the Warburg resistance. The semicircle's diameter gives the charge transfer resistance (R_{ct}), generated by the redox reactions at the electrode–electrolyte interface. R_{ct} values for U-CN and T-CN samples are 1.3 and 1 Ω, respectively. The X-intercept of Nyquist plots can be used to calculate the equivalent series resistance (ESR), which includes the resistance of the KOH electrolyte, the intrinsic resistance of the electrode material, and the resistance at the interface between the electrode and current collector, and the ESR values for U-CN and T-CN samples are 2.5 Ω and 2.2 Ω, respectively [27, 28].

Conclusion

U-CN and T-CN nanosheets were synthesized through the polycondensation method and supercapacitor electrodes were fabricated using the electrophoretic method. Thiourea acts as the source of sulfur for doping. Comparing the supercapacitor performance, T-CN has the highest capacitance of 566 F/g at 3 mV/s. The energy density of the T-CN sample is 41 Wh/kg at a power density of 2.2 kW/kg. Sulfur-doped g-C_3N_4 has enormous potential in the field of electrochemical storage devices.

Author contributions Vattakkoval Nisha contributed toward conceptualization; data curation; formal analysis; original draft; and writing. Padinjare Veetil Salija and Manjacheri Kuppadakkath Ranjusha contributed toward conceptualization and writing. Anjali Paravannoor contributed toward writing and review and editing. M. Neethu Raveendran contributed toward resources. Fabeena Jahan Jaleel contributed toward resources. Baiju Kizhakkekilikoodayil Vijayan contributed toward funding acquisition; investigation; methodology; project administration; software; supervision; visualization; and review and editing.

Data availability Data sets generated during the current study are available from the corresponding author on reasonable request.

Declarations

Competing interests There are no competing interests to declare.

References

1. W. Deng, Y. Zhang, L. Yang, Y. Tan, M. Ma, Q. Xie, RSC Adv. **5**, 13046 (2015). https://doi.org/10.1039/C4RA14820G
2. H.L. Zhu, Y.Q. Zheng, Electrochim. Acta **265**, 372 (2018). https://doi.org/10.20964/2019.07.72
3. G. Nabi, A. Siddiqa, A. Dahshan, M. Tanveer, W. Ali, S. Muzaffar, Diam. Relat. Mater. **145**, 111127 (2024). https://doi.org/10.1016/j.diamond.2024.111127
4. A. González, E. Goikolea, J.A. Barrena, R. Mysyk, Renew. Sustain. Energy Rev. **58**, 1189 (2016). https://doi.org/10.1016/j.rser.2015.12.249
5. Z.S. Iro, C. Subramani, S.S. Dash, Int. J. Electrochem. Sci. **11**, 10628 (2016). https://doi.org/10.20964/2016.12.50
6. M.G. Ashritha, K. Hareesh, J. Energy Storage. **32**, 101840 (2020). https://doi.org/10.1016/j.est.2020.101840
7. J. Safaei, N.A. Mohamed, M.F. Noh, M.F. Soh, N.A. Ludin, M.A. Ibrahim, W.N. Isahak, M.A. Teridi, J. Mater. Chem. A. **6**, 22346 (2018). https://doi.org/10.1039/C8TA08001A
8. R. Arora, M. Dhanda, R. Malik, S. Ahlawat, M. Yadav, S.P. Nehra, S. Lata, Eur. Polym. J. **201**, 112552 (2023). https://doi.org/10.1016/j.eurpolymj.2023.112552
9. Y. Wang, L. Liu, T. Ma, Y. Zhang, H. Huang, Adv. Funct. Mater. **34**, 2102540 (2021). https://doi.org/10.1002/adfm.202102540
10. L. Liu, J. Wang, C. Wang, G. Wang, Appl. Surf. Sci. **390**, 303 (2016). https://doi.org/10.1016/j.apsusc.2016.08.093
11. C. Lu, D. Wang, J. Zhao, S. Han, W. Chen, Adv. Funct. Mater. **27**, 1606219 (2017). https://doi.org/10.1002/adfm.201606219
12. Q. Cao, B. Kumru, M. Antonietti, B.V. Schmidt, Mater. Horiz. **3**, 762 (2020). https://doi.org/10.1039/C9MH01497G
13. C. Shen, R. Li, L. Yan, Y. Shi, H. Guo, J. Zhang, Y. Lin, Z. Zhang, Y. Gong, L. Niu, Appl. Surf. Sci. **455**, 841 (2018). https://doi.org/10.1016/j.apsusc.2018.06.065
14. S. Shaheen Shah, S.M. Abu Nayem, N. Sultana, A.J. Saleh Ahammad, M. Abdul Aziz, Chem. Sustain. Chem. **15**, 20 (2022). https://doi.org/10.1002/cssc.202101282
15. J.S. Ma, H. Yang, S. Kubendhiran, L.Y. Lin, J. Alloys Compd. **903**, 163972 (2022). https://doi.org/10.1016/j.jallcom.2022.163972
16. D. Jiang, L. Chen, J. Zhu, M. Chen, W. Shi, J. Xie, Dalton Trans. **42**, 15726 (2013). https://doi.org/10.1039/C3DT52008K
17. Y. Zheng, Z. Zhang, C. Li, J. Photochem. Photobiol. A **332**, 32 (2017). https://doi.org/10.1016/j.jphotochem.2016.08.005
18. V. Nisha, S. Moolayadukkam, A. Paravannoor, D. Panoth, Y.H. Chang, S. Palantavida, S.J. Hinder, S.C. Pillai, B.K. Vijayan,

Inorg. Chem. Commun. **142**, 109598 (2022). https://doi.org/10.1016/j.inoche.2022.109598
19. X. Cai, J. He, L. Chen, K. Chen, Y. Li, K. Zhang, Z. Jin, J. Liu, C. Wang, X. Wang, L. Kong, Chemosphere **171**, 192 (2017). https://doi.org/10.1016/j.chemosphere.2016.12.073
20. C. Rajkumar, P. Veerakumar, S.M. Chen, B. Thirumalraj, K.C. Lin, ACS Sustain. Chem. Eng. **6**, 16021 (2018). https://doi.org/10.1021/acssuschemeng.8b02041
21. K. Guan, J. Li, W. Lei, H. Wang, Z. Tong, Q. Jia, H. Zhang, S. Zhang, J. Materiomics. **7**, 1131 (2021). https://doi.org/10.1016/j.jmat.2021.01.008
22. G. Zhang, J. Zhang, M. Zhang, X. Wang, J. Mater. Chem. **22**, 8083 (2012). https://doi.org/10.1039/C2JM00097K
23. H. Wang, Y. Liu, L. Kong, Z. Xu, X. Shen, S. Premlatha, J. Energy Storage. **63**, 106935 (2023). https://doi.org/10.1016/j.est.2023.106935
24. H. Guo, Z. Shu, D. Chen, Y. Tan, J. Zhou, F. Meng, T. Li, Chem. Phys. **533**, 110714 (2020). https://doi.org/10.1016/j.chemphys.2020.110714
25. Y. Cui, M. Li, H. Wang, C. Yang, S. Meng, F. Chen, Sep. Purif. Technol. **199**, 251 (2018). https://doi.org/10.1016/j.seppur.2018.01.037
26. H. Lv, Y. Huang, R.T. Koodali, G. Liu, Y. Zeng, Q. Meng, M. Yuan, ACS Appl. Mater. Interfaces **12**, 12656 (2020). https://doi.org/10.1021/acsami.9b19057
27. L. Ma, H. Fan, K. Fu, Y. Zhao, ChemistrySelect **1**, 3730 (2016). https://doi.org/10.1002/slct.201601053
28. V. Nisha, A. Paravannoor, D. Panoth, S.T. Manikkoth, K.M. Thulasi, S. Palantavida, B.K. Vijayan, Bull. Mater. Sci. **44**, 1 (2021). https://doi.org/10.1007/s12034-021-02392-8

Tuijin Jishu/Journal of Propulsion Technology
ISSN: 1001-4055
Vol. 44 No. 3 (2023)

Reinventing Work Nature: The Changing Work Landscape in Malayalam Architecture Magazines in the Post-COVID-19 Pandemic Era

Previn. P. F.
Research Scholar, Christ University, Bangalore & Assistant Professor, Communication And Journalism Dept.
Ses College, Sreekandapuram

***Abstract*:**
The COVID-19 pandemic has profoundly impacted various industries, including the field of architecture magazines. This study aims to analyze the ramifications of the pandemic on the work nature of architecture magazines, with particular attention given to the editorial, business, and mechanical departments. By utilizing a qualitative research approach involving in-depth interviews with experts, this research investigates the changes that have transpired within the nature of work in architecture magazines as a direct response to the pandemic. Many changes have occurred. Findings from this study contribute to a deeper understanding of the changes and transformations within the architecture magazine industry, shedding light on the evolving work nature, strategies, and practices in the post-pandemic era. The insights gained will inform the key players such as stakeholders and advertisers to navigate the multifaceted challenges within the media landscape, reinforcing the resilience of magazine organizations and paving the way for sustained growth in the future.

Keywords: *architecture magazines, COVID-19, editorial changes, business transformation, web-based marketing, digital circulation.*

Introduction

The COVID-19 pandemic, which emerged in early 2020, had profound and far-reaching consequences across various sectors of the Indian economy. Stringent lockdown measures, social distancing protocols, and the swift transition to remote work compelled organizations and employees to adapt to unprecedented circumstances, leading to significant transformations in the nature of jobs in India. This research article aims to explore the extent and implications of these changes, providing insights into key trends and offering valuable perspectives on the future of work.

The pandemic acted as a catalyst, redefining the dynamics of interactions and operations between employees and organizations. The 'State of Remote Work 2022 Report' by Owl Labs revealed a significant increase in interest for remote work by 24% and hybrid work by 16% compared to previous years, while interest in in-office work experienced a decline of 24%. Even after a return to in-office work, a substantial majority of respondents (57%) expressed a preference for full-time remote work. These statistics underscore the profound impact of the pandemic on work preferences and the growing acceptance of remote work arrangements (Owllabs, 2022).

The future of work has been shaped by the rapid adoption of remote work. A survey conducted by Gartner in 2021 revealed that an astonishing 88% of organizations worldwide mandated or encouraged remote work during the peak of the pandemic. This sudden transition necessitated the development of new communication protocols, virtual collaboration tools, and management strategies to effectively support remote teams. Platforms like Slack witnessed a notable 56% increase in usage, highlighting the indispensable role of digital communication tools in enabling remote work (Gartner, 2021).

Remote work also had a positive impact on employee happiness and work-life balance. The Future of Remote Work Report (2022) by Zapier emphasized that remote work allows employees to maintain a satisfactory work-life balance, leading to higher contentment. In fact, 96% of remote workers acknowledged the crucial role work-life balance played in their overall happiness within their professional roles. This shift in focus from rigid office hours to flexible work arrangements has implications beyond the workplace, influencing employees' overall lifestyles and well-being (Future Workplace, 2022).

The nature of jobs underwent a significant transformation across various industries. Sectors like healthcare, e-commerce, and online education experienced an unprecedented surge in demand, leading to the emergence of new job roles and opportunities. For instance, telemedicine visits in the United States alone saw a remarkable 72% increase in 2020, necessitating the hiring of additional healthcare professionals and support staff to cater to the rising demand for virtual healthcare services. On the other hand, sectors heavily reliant on physical presence, such as hospitality, travel, and retail, encountered substantial disruptions, resulting in a significant decline in employment, with an estimated 8.8% decrease in global working hours according to the International Labour Organization (ILO).

The pandemic's impact necessitated a reevaluation of job roles and the acquisition of new skills. Organizations recognized the need to upskill their workforce to adapt to the changing business landscape. Digital skills such as data analysis, coding, and cybersecurity were in high demand. Online educational platforms played a crucial role in skill development during lockdowns, providing individuals with opportunities to enhance their skillsets and human capital.

The shift to remote work also brought about increased reliance on digital technologies. A significant rise in internet usage was observed during the pandemic, with a 13% increase in broadband subscribers in India in 2020 alone, as per the Telecom Regulatory Authority of India (TRAI) (Indbiz, 2020). This digital transformation facilitated seamless information transfer, communication, and collaboration among employees, revolutionizing traditional work processes and enabling virtual teamwork across geographical boundaries.

Despite the advantages of remote work, it also presented challenges in maintaining work-life balance. A survey conducted by Ernst & Young (EY) revealed that 57% of Indian employees reported an increase in working hours during the pandemic, leading to heightened stress levels and burnout. This calls for a reassessment of work policies and the implementation of support mechanisms to prioritize employee well-being (Spence, 2020).

In conclusion, the COVID-19 pandemic has triggered transformative changes in work culture and the nature of jobs in India. The widespread adoption of remote work, increased reliance on digital technologies, shifts in job roles and skills, and the impact on work-life balance have reshaped the employment landscape. Understanding these changes is crucial for policymakers, organizations, and individuals to effectively navigate the future of work. The examples and statistics presented in this article highlight the profound impact of the pandemic and the need for continuous adaptation and upskilling to thrive in the evolving work environment. Further research and industry-specific studies are necessary to gain a deeper understanding of transformations within specific sectors, such as the media sector, in response to the pandemic. By learning from these experiences, we can better prepare for future challenges and opportunities in the dynamic world of work.

Review Literature

The COVID-19 pandemic led to significant changes in work culture, prominently marked by the widespread adoption of remote work and digitalization. FlexJobs (2021) reports that the pandemic accelerated the remote work trend, resulting in a substantial increase in the number of professionals working remotely in India. This transformation was facilitated by advancements in technology and the availability of digital tools and platforms (Narang, 2022). Remote work not only changed the physical work environment but also impacted the way teams collaborate and communicate.

The COVID-19 pandemic emphasized the importance of flexible work arrangements, particularly remote work. Employers now see the benefits of telecommuting and non-traditional work hours, leading to an increase in offering flexible options. These arrangements have long-term benefits like improved recruitment, retention, diversity, ethical behavior, and social responsibility efforts. Employers can also experience advantages such as cost savings, increased productivity, and higher employee engagement. However, implementing flexible work

arrangements can be challenging for some organizations, especially smaller ones lacking the necessary resources (Shrm, 2023).

The transition from a pandemic to an endemic state is causing a significant shift in the working culture. The new focus revolves around three essential keywords: health, safety, and flexibility. These factors are now at the forefront of shaping the way of work (Tarigan, Mannan, & Uddin, 2022).

The Covid-19 pandemic rapidly reshaped workplace culture, highlighting the potential of remote work and questioning the significance of in-person interactions. Organizational leaders must now determine which cultural changes to embrace and address during the recovery phase. The widespread adoption of digital tools necessitates clear direction and regular check-ins. Addressing social isolation and hidden costs of remote work becomes essential, prioritizing mental health awareness and setting boundaries. As the pandemic subsides, leaders should assess positive behavioral shifts to reinforce for the future. By reflecting and taking deliberate action, they can seize opportunities for positive transformation and growth (Thomas, 2020).

The paper titled "A study of work-culture changes at post Covid-19 pandemic in Greater Jakarta" examines the impact of the Covid-19 pandemic on workplace culture in the Greater Jakarta area. The study finds that many companies implemented work-from-home policies during the pandemic, which resulted in successful employee safety and performance. As the pandemic transitions to an endemic phase, the study identifies health, safety, and flexibility as keywords for the new working culture. The research indicates that companies have adopted different working models, with 66% working from the office, 30% in a hybrid system, 2% entirely from home, and 2% from anywhere. The study emphasizes the acceleration of digital transformation and the importance of hybrid working arrangements in the post-pandemic workplace (Tarigan et al., 2022).

The COVID-19 pandemic has led to significant shifts in work culture worldwide, with remote work becoming the new norm for many organizations. This change has challenged traditional office-based work and highlighted the importance of a well-implemented organizational culture in promoting productivity and positive employee experiences (Waisfisz & Hofstede, 2017). Companies have been forced to innovate and pivot their workplace strategies to adapt to remote work practices. While remote work has shown its benefits, it has also posed challenges in maintaining a connected and engaged workforce. To sustain a strong work culture, companies have had to adapt their communication strategies and provide support to remote employees. The pandemic's impact has not been uniform, revealing a gender divide in the workforce, with women facing higher unemployment rates and increased responsibilities for unpaid childcare and household chores (Huen & Bobby, 2020).

The adoption of remote work has led to a shift in work dynamics, with many companies moving towards hybrid work models to offer employees greater flexibility in their work arrangements (Sharma, 2020). This transition highlights the importance of maintaining a strong and sustainable work culture. However, companies must address challenges in establishing fairness and equity among employees in hybrid work settings and retaining talent while providing flexibility (Nickson & Suzy, 2004). Technology has played a significant role in facilitating virtual workspaces and communication among remote teams. Offices are transitioning to a hybrid workspace model, accommodating employees' preferences for remote work. Nevertheless, ensuring equitable growth remains a concern, as certain sectors face job losses while others enjoy work-from-home privileges (Gautam, 2020).

The COVID-19 pandemic has brought about significant disruptions in various industries, including the Media and Entertainment sector, leading to the emergence of a new era termed "Post-COVID media" or "Covidization of Media Industry" (Abdulzaher, 2021). This transformation has been characterized by the adoption of new patterns, tools, roles, and skills in content creation and delivery to reach the target audience effectively.

Creating New Patterns in the Media Content: The pandemic has significantly impacted consumer behavior, prompting global media companies to focus on new digital business models like Video-on-Demand (VOD) content and subscriptions, moving away from a sole reliance on advertising (Netflix report, July 2020). Streaming sites, such as Netflix and Disney+, have experienced a surge in subscribers during the pandemic. The increased data consumption and rise in fixed broadband connections have accelerated the growth of the video streaming segment (Alexander, 2021). Rapid adoption of smartphones, cloud-based services, and incorporation of AI and machine learning have facilitated personalized content recommendations for individual users (Global Media Streaming Market Report, 2021).

Creating New Tools and Solutions for "Media Channels" to Reach the Target Audience: The pandemic has spurred the emergence of innovative tools and technologies to reach the target audience efficiently (Sidhu, 2021). Increased usage of combined data consumption, upgraded infrastructure like 5G technology, and partnerships to offer region-specific content have been observed (Sidhu, 2021). The pandemic has also accelerated creative innovation, leading to new programming formats and workflows (Sidhu, 2021). Covidization of Media Industry will increase media technology investment, which will facilitate access to the target audience with improved efficiency and content quality (Abdulzaher, 2021).

To cope with the Covidization of Media Industry, journalists' skills have adapted, requiring expertise in data analysis, AI journalism, and utilizing technology to address the challenges posed by the pandemic (Abdulzaher, 2021).

The Covidization of Media Industry has marked a significant shift in the media landscape, leading to a future that is more prepared, innovative, and focused on addressing global crises. As media companies continue to adapt and evolve, they must leverage new technologies, data-driven insights, and content personalization to thrive in the Post-COVID media era.

The pandemic influenced printing processes in the magazine publication industry. Organizations adjusted printing schedules and operations to prioritize digital publishing. Printers explored cost optimization measures and automation technologies to streamline printing processes (Malhotra, 2022).

In their study, Jabagi et al. (2019) highlight that the current uncertainty in traditional employment relationships arising due to the ongoing pandemic implicates further consideration for organizations to expand the share of gig workers post-COVID-19 to achieve agility in scaling their workforce up and down as per the business needs. The authors propose a blended model that embodies a new mode of assignment or need-based hiring, wherein organizations engage independent workers with full-time employees to create a team via various platforms. Embracing this approach offers organizations the prospect of achieving enhanced agility in workforce management, thereby addressing the challenges posed by the dynamic and uncertain business landscape (Mahato, Kumar, & Jena, 2021).

The rationale of the Study

The COVID-19 pandemic profoundly impacted the magazine industry, leading to changes in its editorial, business, and mechanical departments. Understanding these changes is crucial as it provides insights into magazine organizations' adaptations and strategies to navigate the pandemic challenges. Examining remote work's influence on content creation and focus in the editorial department, shifts in advertising strategies, revenue generation, and new business models in the business department, and changes in production and distribution methods in the mechanical department helps understand the industry's resilience. Investigating these patterns of work in response to the pandemic informs effective strategies for future crises, contributing to the magazine industry's sustainability and success.

Research Gap

Despite extensive studies on the changes that occurred in the media sector after the COVID-19 outbreak, there is a notable gap in the literature regarding the context of specialized magazines. Specifically, limited research has been conducted on the changes that have transpired in the sector of architecture magazines in Kerala. This research gap presents an opportunity to delve into the transformations that have taken place within specialized magazines, enabling a comprehensive understanding of the changes in the field. By analyzing the changes that have occurred in the sector of architecture magazines in Kerala, this research aims to fill the existing gap in the literature. The study will shed light on the specific adaptations and innovations undertaken by architecture magazines in response to the pandemic. By examining this context, the researcher seeks to provide valuable insights that can be generalized to the broader realm of specialized magazines. Through a thorough analysis of the changes and their implications, the research will contribute to a more comprehensive understanding of the evolving landscape of specialized magazines in the post-COVID-19 era.

Objectives of the Study

The study aims to achieve the following objectives:

To analyze the changes in editorial practices and design of architecture magazines in response to the COVID-19 pandemic.

To examine the emergence of new strategies in circulation and advertising within the architecture magazine sector.

To determine the transformation that has occurred in the production process of architecture magazines.

Methodology

This qualitative study investigates changes in the architecture magazine industry using in-depth interviews with eight experts, including a managing director, CEO, editors, designers, marketing manager, marketing executive, and administrative staff member. The interviews aim to gather rich information about changes in reporting, designing, circulation, advertising, and production processes in response to the COVID-19 pandemic. The study provides a comprehensive analysis of the industry's strategies and experiences during this challenging period. By employing this methodological approach, the research aims to uncover and understand the architecture magazine industry's various transformations in the face of the pandemic.

Findings

The COVID-19 pandemic has brought about significant changes in work culture across various industries, including magazine publication. The findings try to explore the transformations that have occurred in editorial processes, circulation strategies and business aspects such as advertising, and printing within the magazine publication sector.

Editorial

Amidst the COVID-19 pandemic, architecture magazines underwent profound changes in their production and editorial sections. Traditional architecture reporting, reliant on experiential writing and on-site experiences, shifted to armchair journalism due to limitations. To maintain engagement, journalists embraced live interactions with architects and clients through ICT-enabled tools, preserving the essence of architectural spaces. This innovative approach aimed to compensate for the disruption and restore the soul of architecture reporting in the face of pandemic challenges.

The design of architecture magazines underwent significant changes. Reduced advertisements allowed designers greater creative freedom, leading to the incorporation of novel design concepts, spread photographs, whitespaces, artistic boxes, vibrant colors, and captivating illustrations that revitalized the visual appeal and enhanced reader engagement.

Web-based magazines (Webzines), revolutionized the editorial landscape by prioritizing photographs over text. Descriptive captions under images allowed readers to engage deeply with architectural projects, while word limits promoted concise and impactful content. Webzine editors introduced word limits, typically ranging from 350 to 500 words per article, encouraging concise yet impactful content that complemented the visual narrative.

Photography practices underwent a significant transformation during the pandemic. The customary practice of organizing photo shoots by reporters or in-house/freelance photographers was disrupted. Instead, architects, designers, and clients themselves took the initiative to arrange for photographers. During the pandemic, an intriguing development emerged in photography. The architects transformed into skilled photographers. They captured images of their own and others' projects, infusing unique perspective es and personal touches into architectural photography.

Graphic designers shifted to remote work, collaborating with sub-editors through web platforms for efficient review and incorporation of corrections. Editors ensured the magazine's highest standards.

Marketing and Circulation

The COVID-19 pandemic impacted architecture magazine revenues, necessitating business strategy transformation. Measures included launching web editions to attract a wider online audience, offering digital subscriptions, and leveraging social media, websites, and WhatsApp distribution of PDF copies. Architecture magazines adopted Magzter, a digital newsstand, for distribution, gaining access to a wider audience. They earn a percentage of revenue from Magzter subscriptions.

Architecture magazines optimized advertising with a single-pack ad strategy, enabling advertisers to reach multiple platforms (print, webzines, websites, exhibitions). Webzines offered cost-effective options with their lower production costs compared to print editions. Webzines offered additional discounts for advertising. By diversifying revenue streams through web-based marketing, cost-effective advertising, and Magzter distribution, architecture magazines aimed to optimize their revenue potential in the post-COVID-19 era.

Mechanical

A significant development in the architecture magazine industry is the reduction in print editions as digital platforms become more prevalent. With the disruption in global supply chains during the pandemic, the reliance on glossy paper imported from China for printing has decreased, leading to a shift towards Indian paper as an alternative. However, this change has resulted in increased production costs for architecture magazines. To overcome these challenges, magazines are increasingly focusing on web editions, offering benefits such as reduced expenses, broader readership, and the ability to adapt content to evolving audience preferences. The transformation towards online content dissemination reflects the industry's response to changing readership behaviors and financial constraints caused by the pandemic.

Conclusion

This research reveals the profound impact of the COVID-19 pandemic on the architecture magazine industry. Armchair journalism and ICT-enabled tools enabled journalists to engage with architects and designers. Webzines revolutionized content presentation, focusing on captivating photographs and concise descriptions for deeper reader connections. Architectural photography evolved as architects showcased their skills. Remote collaboration streamlined production workflows. New revenue-generation strategies included web-based marketing, web editions, and single-pack ad strategies. These changes have left a lasting impact, showcasing the industry's resilience and adaptability. The findings provide valuable insights for professionals, scholars, and readers, highlighting how the architectural journalism landscape navigated unprecedented challenges during the pandemic. In summary, this research provides a comprehensive understanding of how the architecture magazine industry underwent significant transformations during the COVID-19 pandemic. From adopting new editorial practices to revolutionizing the presentation of content and exploring novel revenue-generation avenues, these adaptations have had lasting impacts on the field. The findings offer valuable insights for industry professionals, scholars, and readers alike, shedding light on the resilience and adaptability of the architectural journalism landscape in the face of unprecedented challenges.

References

[1] Collaboration Hub. (2023). https://pumble.com/learn/collaboration/remote-work-statistics/. Retrieved from pumble.com: https://pumble.com/learn/collaboration/remote-work-statistics/

[2] Abdulzaher, M. (2021). How COVID-19 has Disrupted and Readjusted the Media and Entertainment Industry, by Creating New Roles, Patterns and Skills? Retrieved from: alehttps://aijournalism.net/covidization-of-media-industry/

[3] Future Workplace. (2022). Digital Workplace Trends 2022. Retrieved from https://sequre.app/blog/future-workplace-digital-workplace-trends-2022/

[4] Gartner. (2021, August 23). Gartner survey reveals 44 percent rise in workers' use of collaboration tools since 2019. Press release. Retrieved from https://www.gartner.com/en/newsroom/press-releases/2021-08-23-gartner-survey-reveals-44-percent-rise-in-workers-use-of-collaboration-tools-since-2019

[5] Gautam, A. (2020). Post-Covid: Transformation in Work Culture. Times of India. Retrieved from https://timesofindia.indiatimes.com/readersblog/post-covid-19-impact-on-workingculture/postcovidtransformation-in-work-culture-18804/

[6] Hamingson, N. (2023, April 12). Communication Technology and Inclusion Will Shape the Future of Remote Work. DNB & Business daily.com. Retrieved from https://www.businessnewsdaily.com/8156-future-of-remote-work.html

[7] Huen, B. (2020). COVID-19: Here's How One Pandemic Will Change Our Lives, Forever. ZDNet. Retrieved from www.zdnet.com/article/covid-19-how-one-pandemic-will-change-ourlives-forever/
[8] Indbiz. (2020). India evolving into digital India amidst COVID-19. Retrieved from https://indbiz.gov.in/india-evolving-into-digital-india-amidst-covid-19/
[9] Alexander, J. (2021, March 9). Disney Plus surpasses 100 million subscribers after less than a year and a half. The verge. Report.
[10] Sidhu, J. (2021, August). 4 things to know about the future of media and entertainment. World Economic Forum.
[11] Mahato, M., Kumar, N., & Jena, L. (2021, July). Re-thinking gig economy in conventional workforce post-COVID 19: A blended approach for upholding fair balance. Journal of Work-Applied Management, 1-27. doi:10.1108/JWAM-05-2021-0037
[12] Malhotra, K. (2022). Digital Printing In The 'Post Covid Digital Era'. Retrieved from https://www.print-publishing.com/: https://www.print-publishing.com/10071/digital-printing-in-the-post-covid-digital-era/
[13] Narang, S. M. (2022). Digital Economy and Work-from-Home: The Rise of Home Offices Amidst the COVID-19 Outbreak in India. Journal of the Knowledge Economy, 924-945. doi:10.1007/s13132-022-00896-0
[14] Netflix report. (2020, July).
[15] Nickson, D., & Suzy, S. (2004). Remote Working: Linking People and Organizations. Elsevier Butterworth-Heinemann.
[16] Owllabs. (2022). Retrieved from Owllabs: https://owllabs.com/state-of-remote-work/2022
[17] Paulas, P. B., & Kenworthy, J. B. (2019). Effective brainstorming. In The Oxford Handbook of Group Creativity and Innovation (pp. 287-305).
[18] People Matters. (2020). Looking at the Workplace Post Lockdown. Retrieved from www.peoplematters.in/article/c-suite/looking-at-the-workplace-post-lockdown-25432
[19] Sharma, A. (2020). Looking at the Workplace Post Lockdown. People Matters. Retrieved from www.peoplematters.in/article/c-suite/looking-at-the-workplace-post-lockdown-25432
[20] Spence, P. (2020, July 29). Health. Retrieved from ey: https://www.ey.com/en_gl/health/how-covid-19-reshapes-the-mental-health-needs-of-workers
[21] Tarigan, S. G., Mannan, K. A., & Uddin, N. (2022). A study of work-culture changes at post Covid-19 pandemic in greater Jakarta. IOP Conference Series: Earth and Environmental Science, 1098(1), 012028. doi:10.1088/1755-1315/1098/1/012028
[22] Thomas, J. (2020). How the pandemic can change workplace culture for the better. Retrieved from https://www.strategyand.pwc.com/: https://www.strategyand.pwc.com/m1/en/articles/2020/how-the-pandemic-can-change-workplace-culture-for-the-better.html
[23] UN Report. COVID-19 and Mental Health and Wellbeing. Retrieved from https://www.un.org/en/coronavirus/mental-health-and-wellbeing
[24] Waisfisz, B., & Hofstede, G. (2017). Constructing the Best Culture to Perform. [PDF]. Creative Commons. Retrieved from https://creativecommons.org/licenses/by-nc-nd/4.0/
[25] World Health Organization. (2020). Coronavirus Disease (COVID-19) Pandemic. Retrieved from www.who.int/emergencies/diseases/novel-coronavirus-2019
[26] Romer, D., & Jamieson, K.H. (2021, April). Patterns of Media Use, Strength of Belief in COVID-19 Conspiracy Theories, and the Prevention of COVID-19 From March to July 2020 in the United States: Survey Study. Journal of Medical Internet Research.
[27] Li, C., & Zafar, H. (2020, June 3). COVID-19 has upended the media industry. World Economic Forum.